Constraints on the depositional age and tectonometamorphic evolution of marbles from the Biharia Nappe System (Apuseni Mountains, Romania)

MARTIN KASPAR REISER[1], RALF SCHUSTER[2], PETER TROPPER[3] and BERNHARD FÜGENSCHUH[1]

[1]Institut für Geologie, Universität Innsbruck, Innrain 52, Bruno Sander Haus, 6020 Innsbruck, Austria;
martin.reiser@uibk.ac.at; bernhard.fuegenschuh@uibk.ac.at
[2]Geologische Bundesanstalt, Neulinggasse 38, 1030 Wien, Austria; ralf.schuster@geologie.ac.at
[3]Institut für Mineralogie und Petrologie, Universität Innsbruck, Innrain 52, Bruno Sander Haus, 6020 Innsbruck, Austria; peter.tropper@uibk.ac.at

Abstract: Basement rocks from the Biharia Nappe System in the Apuseni Mountains comprise several dolomite and calcite marble sequences or lenses which experienced deformation and metamorphic overprint during the Alpine orogeny. New Sr, O and C-isotope data in combination with considerations from the lithological sequences indicate Middle to Late Triassic deposition of calcite marbles from the Vulturese-Belioara Series (Biharia Nappe s.str.). Ductile deformation and large-scale folding of the siliciclastic and carbonatic lithologies is attributed to NW-directed nappe stacking during late Early Cretaceous times (D2). The studied marble sequences experienced a metamorphic overprint under lower greenschist-facies conditions (316–370 °C based on calcite–dolomite geothermometry) during this tectonic event. Other marble sequences from the Biharia Nappe System (i.e. Vidolm and Baia de Arieș nappes) show similarities in the stratigraphic sequence and their isotope signature, together with a comparable structural position close to nappe contact. However, the dataset is not concise enough to allow for a definitive attribution of a Mesozoic origin to other marble sequences than the Vulturese-Belioara Series.

Keywords: marble, Sr-isotope stratigraphy, calcite–dolomite geothermometry, Vulturese-Belioara, Biharia, Dacia, Apuseni Mountains.

Introduction

The Permo–Mesozoic sediments of the Circum-Pannonian region provide important data for palaeogeographic correlations between different Mega-units/Megaterranes in the Alpine–Carpathian–Dinaridic orogenic system (cf. Schmid et al. 2008; Vozár et al. 2010). Surface outcrops in the Apuseni Mountains allow study of the interaction between the Tisza Mega-Unit and the Dacia Mega-Unit, represented by the Biharia Nappe System, during the Alpine evolution.

The Mesozoic sediments of the Tisza Mega-Unit in the Apuseni Mountains experienced no or only slight metamorphic overprint and thus are well correlated with other Permo–Mesozoic sequences in the region (e.g., Kutassy 1928a,b; Patrulius et al. 1971; Lupu 1972; Haas & Péró 2004; Haas et al. 2010; Kovács et al. 2010; Vozárová et al. 2010). The Biharia Nappe System also contains lenses of carbonate and dolomite rocks at different structural levels and often exhibits calcite and dolomite marbles at the contact between the tectonic units (see Fig. 1; Mârza 1965; Lupu 1972). However, due to intense deformation and a pervasive metamorphic overprint during the Cretaceous, the age of these marble sequences is not well constrained.

Thus, this study presents a characterization of the marble sequences within the Biharia Nappe System based on field evidence, Sr-isoto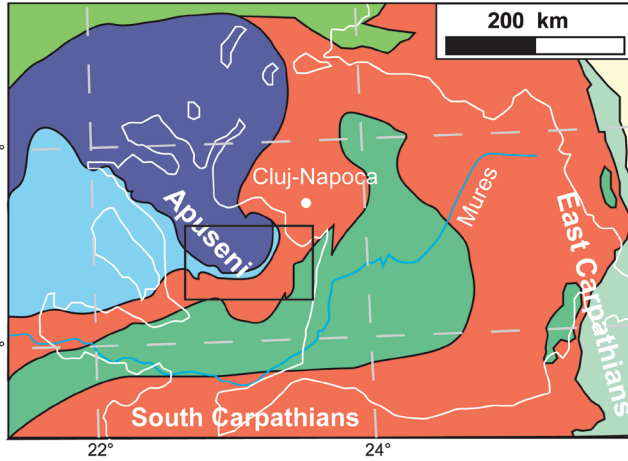pe stratigraphy, calcite–dolomite geothermometry as well as analyses of carbon- and oxygen-isotopy, to allow for their attribution to a Palaeozoic or Mesozoic origin.
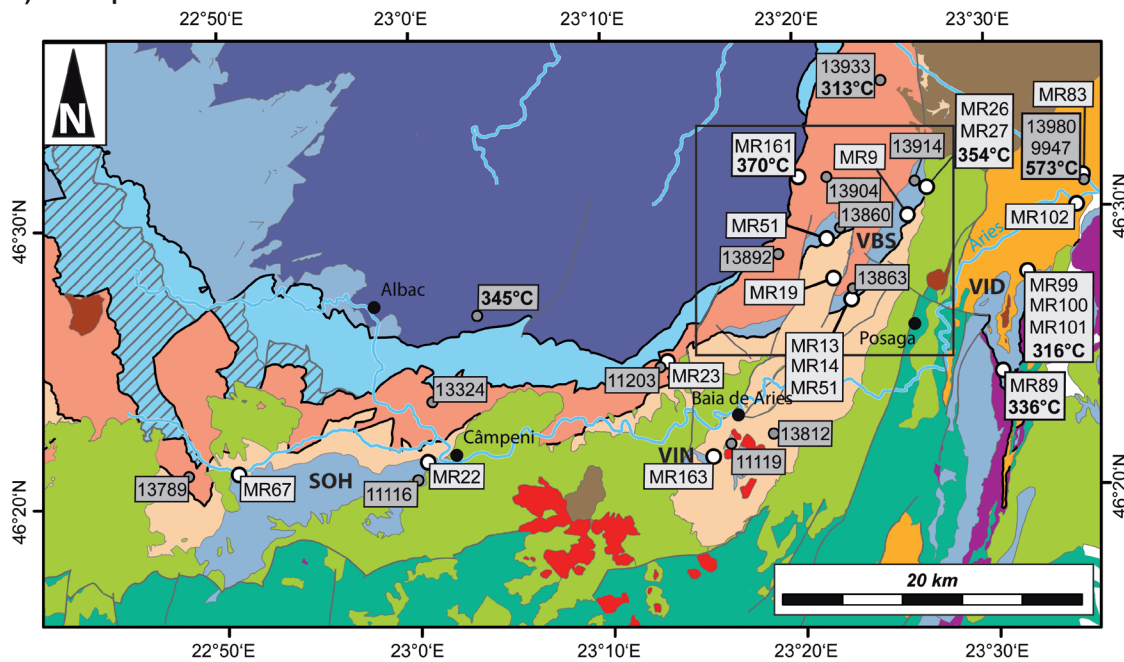
Geological background

Until the Early Jurassic, the Alcapa, Tisza and Dacia Mega-units were located in neighbouring positions, forming the northwestern and northeastern Neotethys margin (e.g., Săndulescu 1984; Vörös 1993; Csontos & Vörös 2004; Haas & Péró 2004; Schmid et al. 2008; Haas et al. 2010; Kovács et al. 2010). The Middle/Late Jurassic eastward propagating opening of the Alpine Tethys starts the separation of the Alcapa, Tisza and Dacia Mega-units from Europe. Vörös (1993) clearly shows a Mid- to Upper Jurassic change from a European to a Mediterranean faunal assemblage through brachiopod taxa (e.g., *Nucleata, Calvirhynchia contraversa*) for both units, namely Tisza and Dacia. It is an ongoing discussion whether the Tisza and Dacia Mega-units were separated by an oceanic branch (e.g., Săndulescu 1984; Schmid et al. 2008; Kounov & Schmid 2013), or whether the two units formed part of the same microplate, which moved and rotated away from the European margin in the Late Jurassic (Csontos & Vörös 2004). Recent results indicate a comparable evolution in both, Tisza and Dacia Mega-units from Early Cretaceous

Fig. 1. a — Overview of the study area, a black square shows the position of the study area in the Alpine–Carpathian–Dinaride orogenic system. Modified from Kounov & Schmid (2013). **b** — Simplified overview map of the Apuseni Mountains. Sample locations and abbreviations of the units described in the text are given; a black frame marks the position of Fig. 2.

times onwards and thus support a neighbouring position throughout their Alpine evolution (Reiser et al. 2016).

Following the Late Jurassic emplacement of the South Apuseni Ophiolites, Early Cretaceous deformation (D1) is shown through structural and thermochronological data (Ar–Ar muscovite and Ar–Ar hornblende; Dallmeyer et al. 1999; Reiser et al. 2016). Subsequent NW-directed thrusting of the Biharia Nappe System on top of the Bihor and Codru Nappe during D2 caused greenschist-facies metamorphic overprint in structurally lower parts of the nappe pile, namely the Bihor Nappe, Codru Nappe, Baia de Arieș Nappe and Biharia Nappe s.str. (cf. Ianovici et al. 1976; Balintoni & Vlad 1996; Kounov & Schmid 2013). This late Early Cretaceous–early Late Cretaceous phase is well constrained through structural and thermochronological data and responsible for the present-day nappe stack of the Apuseni Mountains (Săndulescu 1984; Balintoni 1994b; Schuller 2004; Schuller & Frisch 2006; Schuller et al. 2009; Merten et al. 2011; Kounov & Schmid 2013).

Late Cretaceous extension/exhumation (D3; Reiser et al. 2016) is associated with syn-tectonic hanging wall sedimentation of "Gosau-type" sediments which seal the nappe contacts of previous tectonic events (Schuller 2004; Schuller & Frisch 2006). Compressional deformation during the late Maastrichtian–middle Eocene ("Laramian Phase"; D4) caused brittle reactivation of previous structures (Balintoni 1994b; Merten et al. 2011). Top-NW to N and subordinate top-ESE high-angle thrusts along nappe contacts, N–S striking folds, as well as uplift and erosion of basement and post-tectonic sediments are attributed to this E–W compression (Balintoni 1994b; Krézsek & Bally 2006; Schuller & Frisch 2006; Merten et al. 2011).

The Biharia Nappe System of the Apuseni Mountains comprises pre-Variscan, polyphase metamorphic crystalline basement (Balintoni et al. 2010), Palaeozoic granitoid intrusions, a late Palaeozoic cover, Mesozoic sequences of variable thickness, and Jurassic ophiolites (e.g., Ianovici et al. 1976; Bleahu et al. 1981; Săndulescu 1984; Pană 1998; Balintoni et al. 2009; and detail map in Fig. 1). Syn- to post-tectonic deposits of Early and Late Cretaceous age unconformably overlie the nappe contacts between the Vidolm, the Baia de Arieș and Biharia s.str. nappes (e.g., Bleahu et al. 1981; Csontos & Vörös 2004; Schuller et al. 2009; Kounov & Schmid 2013). Based on the fact that the Transylvanian Ophiolitic unit (which includes the South Apuseni Ophiolites; Hoeck et al. 2009; Ionescu et al. 2009, 2010) overlies the Bucovinian Nappe System and the Biharia Nappe System (cf. Săndulescu 1984; Krézsek & Bally 2006), Schmid et al. (2008) attributed the Biharia Nappe System to the Dacia Mega-Unit, while other authors (e.g., Pană 1998; Csontos & Vörös 2004; Haas & Péró 2004) previously considered it to be an integral part of Tisza.

The Vulturese-Belioara Series (VBS) of the Biharia Nappe s.str. (cf. Mârza 1965, 1969; Ianovici et al. 1976; Balintoni et al. 1987) and the Sohodol Marbles of the Baia de Arieș Nappe (Ianovici et al. 1976; Bordea et al. 1988) are examples of such sequences thought to represent the Mesozoic cover of their respective tectonic units (pers. comm. by Trümpy in Balintoni 1994a). A comparable succession consisting of siliciclastic

sediments, calcite marbles and dolomites is also present in the structurally highest Vidolm Nappe, just below the South Apuseni Ophiolites. Kounov & Schmid (2013) tentatively attributed a Mesozoic age to this succession. Due to their lower erodability, these calcite and dolomite marbles form cliffs within the surrounding basement lithologies.

Marble sequences of the Biharia Nappe System

Vulturese-Belioara Series (VBS) and marbles of the Biharia Nappe s.str.

The greenschist-facies metasedimentary succession of the Vulturese-Belioara Series crops out at the contact between the Biharia Nappe s.str. and the Baia de Arieș Nappe in the south-eastern part of the Apuseni Mountains (cf. Figs. 2, 3a and Mârza 1965, 1969; Ianovici et al. 1976; Balintoni et al. 1987). This sequence of quartzites, dolomites and marbles was traditionally interpreted as the low-grade metamorphosed middle Palaeozoic cover of the medium-grade metamorphic basement, but field observations by Trümpy (pers. comm. reported in Balintoni 1994a) and Sasaran E. (pers. comm.) point towards a deposition during the Triassic. Based on the stratigraphy of the Vulturese-Belioara Series, a correlation with the Föderata-Struženik Series of the Western Carpathians was suggested (Dimitrescu in Ianovici et al. 1976). The Vulturese-Belioara Series comprises the following lithologies: basal quartzitic conglomerates with white and purple quartz-components (Fig. 3b) and sericitic schists; ~100 m of well bedded (0.5–2 m) black graphitic dolomites with remnants of crinoids (pers. comm. by Sasaran E.) passing into ~350 m thick, massive reddish to yellowish dolomites, followed by 0.5–5 m of thin-bedded (0.5–10 cm), red weathered, sericitic and platy marbles (see Fig. 3c) and finally ~350 m thick-bedded light grey, beige and white, partially dolomitic marbles (Fig. 3d, e) at the top. Basal quartzitic conglomerates, dolomites and marbles dip to the SE and are folded around a NE–SW oriented fold axis (Mârza 1965, 1969; Solomon et al. 1981; Ianovici et al. 1976). The fold hinge is not exposed, but the relationship between bedding and axial plane foliation indicates a synform. Two large NNE–SSW trending faults dissect the Vulturese-Belioara Series causing the present-day geometry of three ridges: the Vulturese-Belioara ridge in the NE, the Scarița-Belioara ridge in the centre and the Leurda ridge in the SE (Fig. 4). The bedding planes show a trend towards steeper inclinations towards the SW and their strike changes from NE–SW in the Belioara ridge to ENE–WSW in the Scarița-Belioara ridge (Figs. 2, 3a, 4). A set of roughly N–S to NW–SE trending vertical joints commonly exhibits hematite-limonite ore mineralization. The mineralized joints provide evidence for hydrothermal activity in the Vulturese-Belioara Series, although its age cannot be constrained (Ianovici et al. 1976).

The Ocoliș and Poșaga valley cross the Vulturese-Belioara Series and allow for comparison along two sections (Fig. 5). In the Ocoliș profile only the lower limb of the fold is exposed
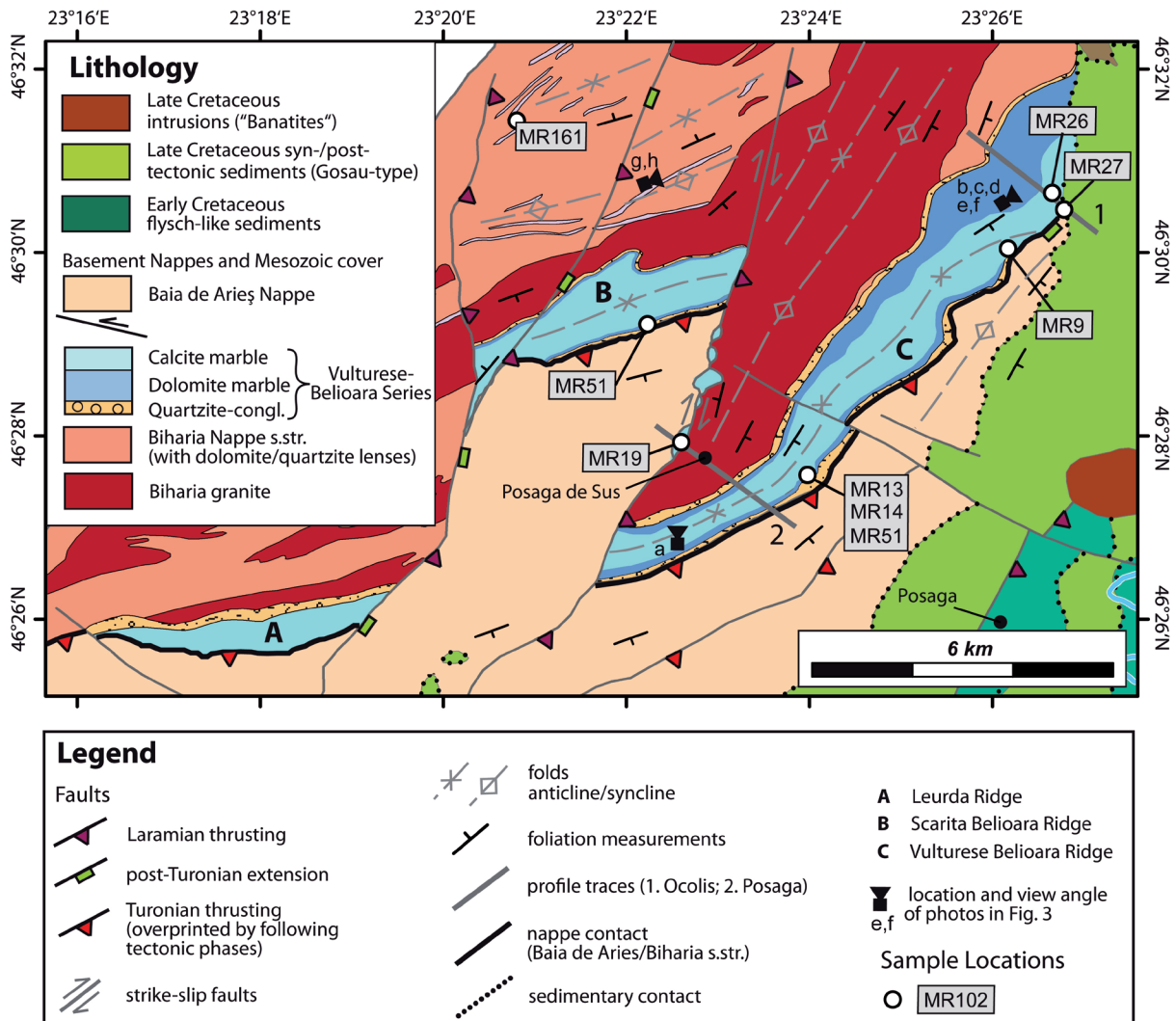
Fig. 2. Geological map of the Vulturese-Belioara Series. Sample locations and profile traces of Fig. 5 are given on the map.

and the calcite marbles and dolomites show a greater thickness compared to the Poşaga profile. At the top of the succession, a thin layer of mylonitized marbles (see Fig. 3e) cut off by a brittle fault associated with fault breccias mark the nappe contact to the overlying Baia de Arieş Nappe. Several NE–SW trending faults, filled with brecciated fragments in a red matrix cut (Fig. 3f) through the marbles towards the top of the succession. The Poşaga Profile exhibits a complete section through the fold: the calcite marbles are located in the core of the fold and the dolomites and quartzitic conglomerate as thin layers on both limbs. The dip of the bedding planes is slightly steeper than in the Ocoliş profile (Fig. 5).

Several dolomite lenses crop out within the crystalline basement rocks in the eastern part of the Biharia Nappe s.str. (Fig. 3g and h). The dolomite is yellowish brown in colour and shows intense cross cutting by quartz veins. Lenses of pinkish white quartzite are often associated with the dolomite. The pattern of these lenses reflects the fold structure of the Biharia Nappe s.str. and seemingly adhere to a continuous structural level (cf. Fig. 2).

Sohodol Marbles and marbles of the Baia de Arieş Nappe

In the western part of the Apuseni Mountains, a sedimentary sequence known as Sohodol Marbles (SOH in Fig. 1) overlies the Baia de Arieş Nappe with a discordant contact (Ianovici et al. 1976; Bordea et al. 1988). Basal black quartzites and graphitic schists are overlain by white to dark-grey, well bedded (10 cm) marbles with strongly folded quartz lenses. These white marbles are intercalated by thin reddish layers. The transition from quartzites to marbles is marked by breccias and cataclasites. The age of this marble succession is not well constrained yet, but according to Ianovici et al. (1976) crinoid stems were described in the Sohodol Marbles by Lupu (1972), indicating a Mesozoic age of the Sohodol Marbles.

In the eastern part of the Baia de Arieş Nappe, near the town of Baia de Arieş, several large marble lenses crop out in the vicinity of Neogene intrusive bodies (VIN in Fig. 1). The age of these coarse grained, white to yellowish marbles is not known, but Kounov & Schmid (2013) tentatively attribute a Mesozoic age in their map of the study area.
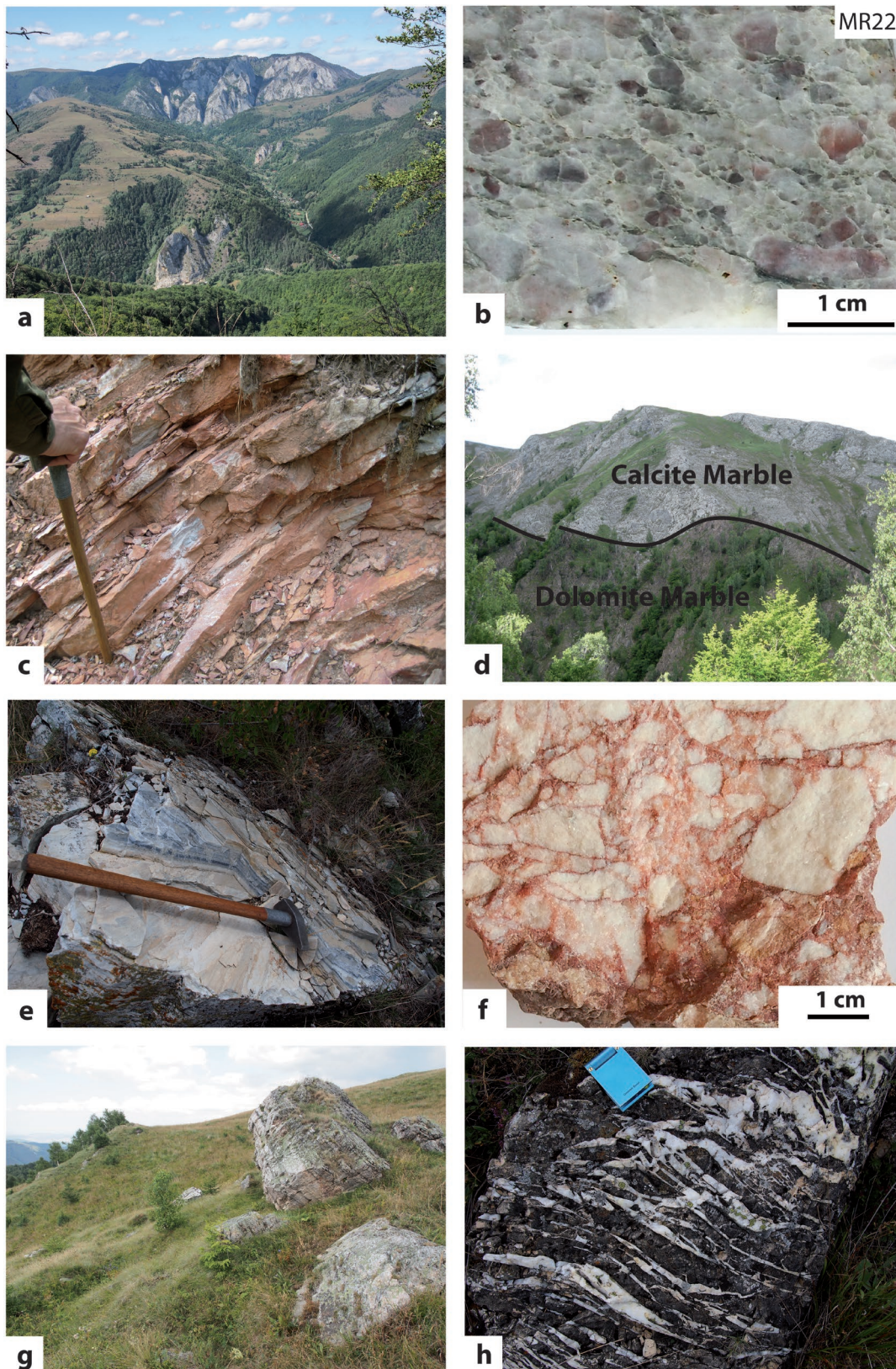
Fig. 3. Field observations, locations are marked in Fig. 2: **a** — the Scariţa-Belioara ridge and isolated marble blocks along the fault, picture was taken towards the north; **b** — polished section of the basal quartz conglomerate with red components; **c** — the red condensed marbles separating the dolomites and calcite marbles; **d** — the contact between dolomites and calcite marbles in the field, picture taken towards the NE; **e** — image of outcrop with typical layered calcite mylonites from which sample MR51 was taken; **f** — fault-breccia with red matrix; **g, h** — isolated quartzite lenses, associated with strongly veined dolomite lenses.
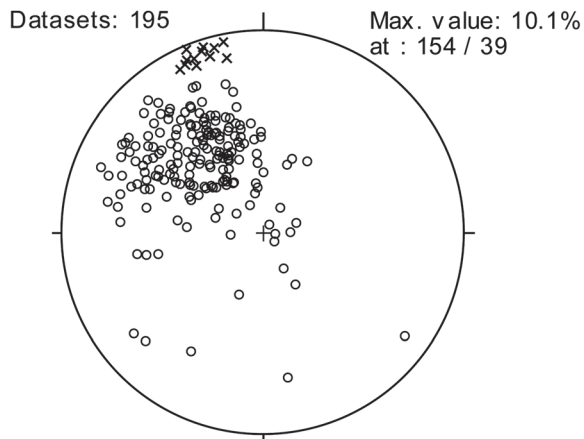
Fig. 4. Pi-plot of bedding planes for the Vulturese-Belioara Series showing a general dip towards the SE. A subset of steeply SSE-dipping bedding planes from the Scarița-Belioara ridge is marked with × symbols.

Marbles of the Vidolm Nappe

Similarly to the Baia de Arieș Nappe, the Vidolm Nappe comprises several occurrences of calcite and dolomite marbles (Fig. 1). Marble lenses are located within basement rocks (e.g., sample MR83) and a sequence of calcite and dolomite marbles is present below the tectonic contact with the overlying South Apuseni Ophiolites (VID in Fig. 1). The marbles at the top of the Vidolm Nappe exhibit basal quartzitic conglomerates ("Meta-Psephites"; Balintoni et al. 1987) and black quartzitic schists (Ianovici et al. 1976). The calcite marbles are grey, metre-scale to cm-scale bedded with phyllitic and quartzitic intercalations, while the overlying dolomite marbles are yellowish-white and massive. At the top of the sequence, light grey marbles are present. The Vidolm Marbles are directly overlain by the South Apuseni ophiolites and their Late Jurassic to Early Cretaceous sedimentary cover, represented by non-/low-metamorphosed shallow-water limestones (Ilie 1936; Sasaran 2005). The marbles exhibit isoclinal folds and increasing deformation towards the contact with the overlying ophiolites. Several dikes with ferruginous crusts cross cut the marbles and vertical joints exhibit ore mineralization. Savu (2007) reports burial-related metamorphism at temperatures from 200–400 °C for marbles in the uppermost part of the Vidolm Nappe. Based on their position on top of the basement rocks, Kounov & Schmid (2013) assume a Mesozoic age of these marbles, but other than that no information on their age is given in published literature.

Methods

Mechanical sample preparation, X-ray fluorescence spectrometry (using a Spectro-Xepos X-ray spectrometer) and O−C isotope analyses were performed at the University of Innsbruck, while the chemical sample preparation for

Sr-isotopic analyses was performed at the Geological Survey of Austria in Vienna. Weathered surfaces were removed from the samples before crushing and milling.

δ¹⁸O and δ¹³C isotopy

Stable isotope ratios from carbonates potentially yield information about their origin, for example, allowing reconstructions on the isotopic composition of the ocean during their deposition. However, processes such as deformation, volatilization, mineral reactions and metasomatism can affect and alter the isotope ratio of the samples. Thus, the source sets an isotopic baseline which can subsequently be shifted by isotopic fractionation. This study provides a general overview of the $\delta^{18}O$ and $\delta^{13}C$ isotopy of the marbles, which is used for comparative purposes. Oxygen and carbon isotope values of several marbles from the Apuseni Mountains were measured to distinguish between altered and original isotopic compositions.

Subsamples for stable carbon and oxygen isotope analyses were obtained using a handheld drill bit after removing the weathered surfaces. Analyses were carried out at the Institute of Geology at the University of Innsbruck, using a Thermofinnigan GasBench II equipped with a CTC Combi-Pal autosampler linked to a DeltaPlusXL mass spectrometer. The analytical precision (1 sigma) is typically 0.08 % for $\delta^{18}O$ and 0.06 % for $\delta^{13}C$ (Spötl & Vennemann 2003). The reaction time is 82 minutes per sample. Carbon stable isotope ratios are reported relative to the VPDB (Vienna-Pee Dee Belemnite). The oxygen stable isotope ratios are given relative to the VPDB and as well in VSMOW (Vienna-Standard Mean Ocean Water).

Calcite−dolomite geothermometry

Calcite−dolomite geothermometry is based on the temperature-dependent miscibility between calcite and dolomite. Increasing temperatures cause X_{mg} in calcite to increase along the calcite-dolomite miscibility gap (Letargo et al. 1995). The following equation by Anovitz and Essene (1987) describes the composition-temperature relation in calcite:

$$T(°K) = A(X_{mg}) + B/(X_{mg})^2 + D(X_{mg})^{0.5} + E$$

A, B, C, D and E are coefficients with the values –2360, –0.01345, 2620, 2608 and 334. X_{mg} represents the concentration of mg in calcite (mg/(mg+ca)) in atoms per formula unit. The formula above does not account for the molar concentration of $FeCO_3$ in calcite. However, due to the low Fe-content of the analysed limestones it is of no concern for the result. The commonly occurring decomposition of dolomite from calcite during cooling makes this geothermometer suitable for low-grade rocks. Due to the high reequilibration-rate during retrograde conditions, the temperature estimates represent the last thermal overprint and have to be considered as minimum temperatures (Essene 1983).
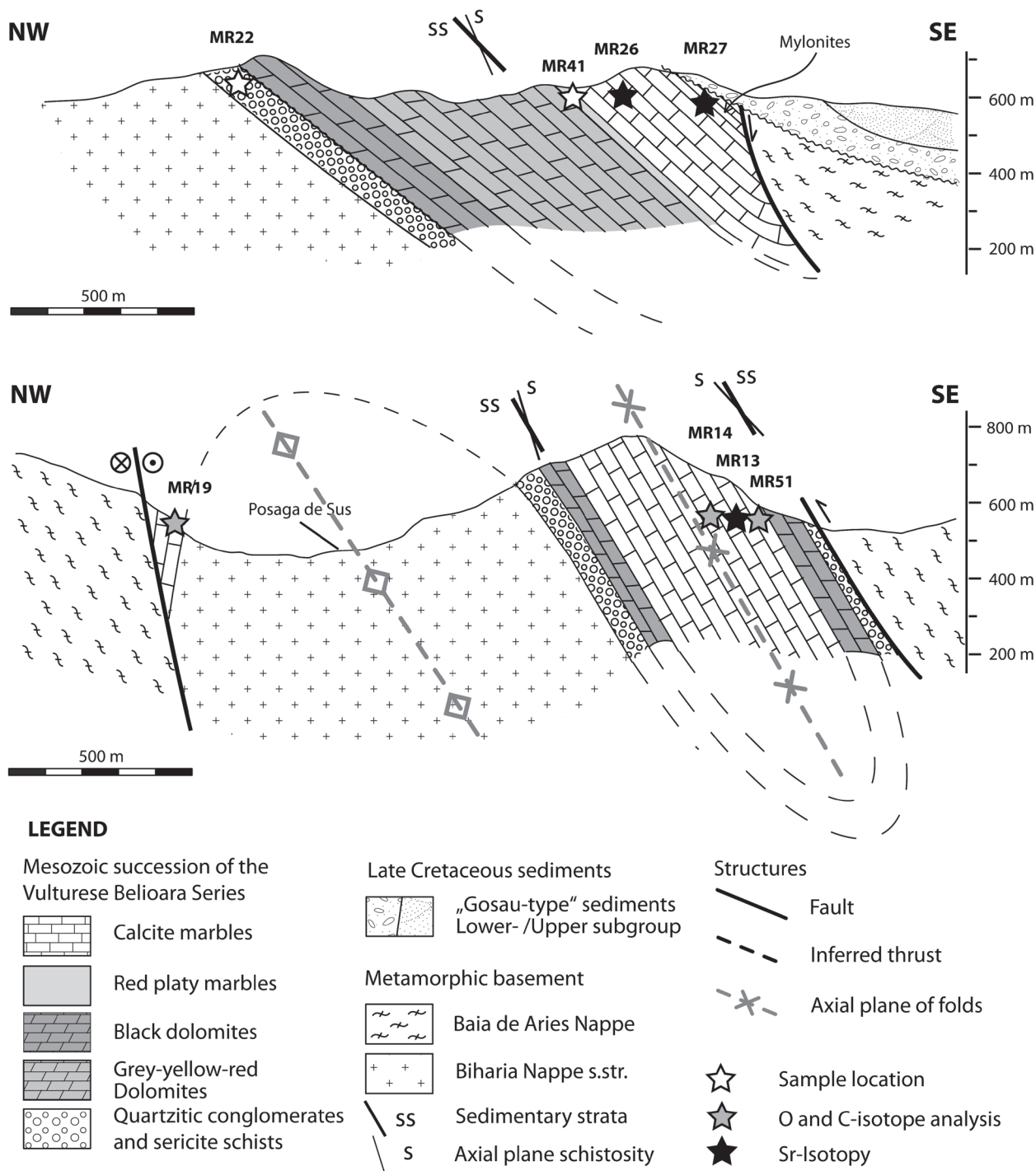
Fig. 5. Profiles through the Vulturese-Belioara Series: Ocoliş-Section (above) and Poşaga-Section (below). For profile trace see Fig. 2.

Sr-isotope stratigraphy

The $^{86}Sr/^{87}Sr$ ratio of dissolved Sr in the world's oceans changes over time and thus allows correlation and dating of sediments using their $^{86}Sr/^{87}Sr$ isotopic ratio (McArthur 1994; Veizer et al. 1997, 1999; McArthur et al. 2012). McArthur et al. (2001, 2004) present a standard curve of $^{86}Sr/^{87}Sr$ variation over the last 509 Ma. The curve represents the best-fit on

measurements of $^{86}Sr/^{87}Sr$ in samples dated by biostratigraphy, magnetostratigraphy and astrochronology enabling the user to do a rapid conversion of $^{86}Sr/^{87}Sr$ to age and vice versa (McArthur et al. 2001). The reliability of Sr-isotope stratigraphy depends on the potential of the tested rocks to preserve depositional isotopic values, but even marbles that have experienced multiphase metamorphism (up to amphibolite-facies conditions) and deformation may retain their depositional

carbon-isotope values and preserve near-primary $^{87}Sr/^{86}Sr$ ratios (Frank et al. 1990; Melezhik 2001, 2013; Satish-Kumar et al. 2008; Murra et al. 2011).

For Sr-isotope analyses, only pure white marble samples from the centre of at least some decimetres wide layers were chosen. The carbonate fractions of most samples were analysed for Mn, Mg, Sr and Ca by X-ray spectroscopy to evaluate the degree of post-sedimentary alteration and to check for Rb contamination (geochemical screening; e.g., Brand & Veizer 1980) according to the criteria of Melezhik et al. 2001. About 70 mg of WR-powder were dissolved in 0.1n CH_3COOH and the un-dissolved part of the sample was extracted by a centrifuge immediately after dissolution of the carbonate. The chemical preparation follows the procedure described by Sölva et al. (2005).

Sr-ratios were analysed on a Triton TI TIMS from Re double filaments. Due to the fact that measurements have been performed over three years, changes in the hardware of the machine caused different values for the NBS987 standard for the individual periods of measurements:

2010 $^{86}Sr/^{87}Sr=0.710252\pm6$ $2\sigma_m$ (n=8)

2011 $^{86}Sr/^{87}Sr=0.710246\pm4$ $2\sigma_m$ (n=10)

2012 $^{86}Sr/^{87}Sr=0.710278\pm3$ $2\sigma_m$ (n=9)

The measured values were corrected for a standard value of 0.710248.

Results

Thin sections

Thin sections of the marbles were investigated under the microscope to study geometrical relationships between the mineral constituents with particular reference to calcite. Homeoblastic and heteroblastic textures were discriminated and the maximum grain size of calcite (MGS) was measured to characterize the marbles. Deformation twins were discriminated to qualitatively determine the degree of metamorphic overprinting. The thin sections are discussed for each nappe within the Biharia Nappe System (Vidolm, Baia de Arieş and Biharia s.str.). In each section the thin sections are discussed from bottom to top: the description starts with marble lenses from the crystalline basement before the marbles at the top of the nappes are discussed. Deformation twins in calcite are used to provide an estimate of the thermal overprint recorded in the calcite marbles (e.g., Jamison & Spang 1976; Ferrill 1991; Burkhard 1993; Ferrill et al. 2004).

Vidolm Nappe

Sample MR83 (Fig. 6a) was taken from a marble lens containing retrogressed eclogite bodies (personal comm. Balintoni I.; Fig. 6b) within the crystalline basement of the Vidolm Nappe. A coarse grained homeoblastic texture indicates a high thermal overprint (amphibolite facies; cf. Pană 1998) with only little retrogressive overprint. However, sericitic rims around mica flakes indicate a polymetamorphic evolution. The thin sections from the top of the Vidolm Nappe exhibit decreasing grain sizes and increasing amounts of dynamically recrystallized grains towards the hanging wall contact with the South Apuseni ophiolites (samples MR101, MR100, MR99 and MR89). Serrated grain boundaries in sample MR101 (Fig. 6c) indicate grain boundary migration recrystallization under thermal conditions of 250–350 °C. Angular feldspars showing undulose extinction support this conclusion (Passchier & Trouw 1996). In combination with the presence of thick and patchy type IV twins which are cross cut by type II and type I twins (sample MR101; Fig. 6c) a polyphase deformation can be inferred (cf. Ferrill et al. 2004).

Baia de Arieş Nappe

Mica flakes in sample MR23 (Fig. 6d) from a dynamically recrystallized dolomite marble lens within the crystalline basement are beginning to form a weak foliation. The predominantly coarse grained samples from the Sohodol Marbles (e.g., sample MR67; Fig. 6e) show grain boundary migration recrystallization and are interpreted to have formed under high anchizonal to lower greenschist facies temperatures (250–350° C). The calcite twins range from patchy type IV twins, bent and serrated thick twins (type III) to thin twins (type I) crosscutting the former (Passchier & Trouw 1996). Thus, a polyphase deformation is inferred. The very coarse grains (2.5 mm) from sample MR163 (Vinţa-marbles) probably relate to a thermal overprint during the intrusion of Neogene magmatics in the vicinity.

Biharia Nappe s.str.

Sample MR51 (Fig. 6f) represents a fine grained, dynamically recrystallized calcite mylonite at the contact between the

Fig. 6. Thin sections of marbles from different tectonic units. **a** — sample MR83 from the Vidolm Nappe, which exhibits tapered twinning lamellae and coarse grained texture (crossed polarizers); **b** — garnet and amphibole minerals under crossed polarizers in a thin section of a presumably retrogressed eclogite (personal comm. Balintoni, I.) associated with the marbles of sample MR83; **c** — thin twinning lamellae overprinting thick and patchy twinning lamellae in sample MR101 from the Vidolm Nappe (crossed polarizers); **d** — heteroblastic texture of sample MR23 from the Baia de Arieş Nappe. The large, dark grey grain in the centre exhibits patchy twins (crossed polarizers); **e** — sample MR67 from the Sohodol marbles of the Baia de Arieş Nappe with coarse grain sizes and multiple generations of twins (crossed polarizers); **f** — fine-grained calcite mylonite of sample MR51 (Vulturese-Belioara Series; Biharia Nappe s.str.); **g** — sample MR27 (Vulturese-Belioara Series; Biharia Nappe s.str.) exhibits triple junctions and patchy type IV twins, (crossed polarizers); **h** — sample MR41 (Vulturese-Belioara Series; Biharia Nappe s.str.) exhibits a heteroblastic texture with small recrystallized grains and patchy type IV twins in larger grains (crossed polarizers).
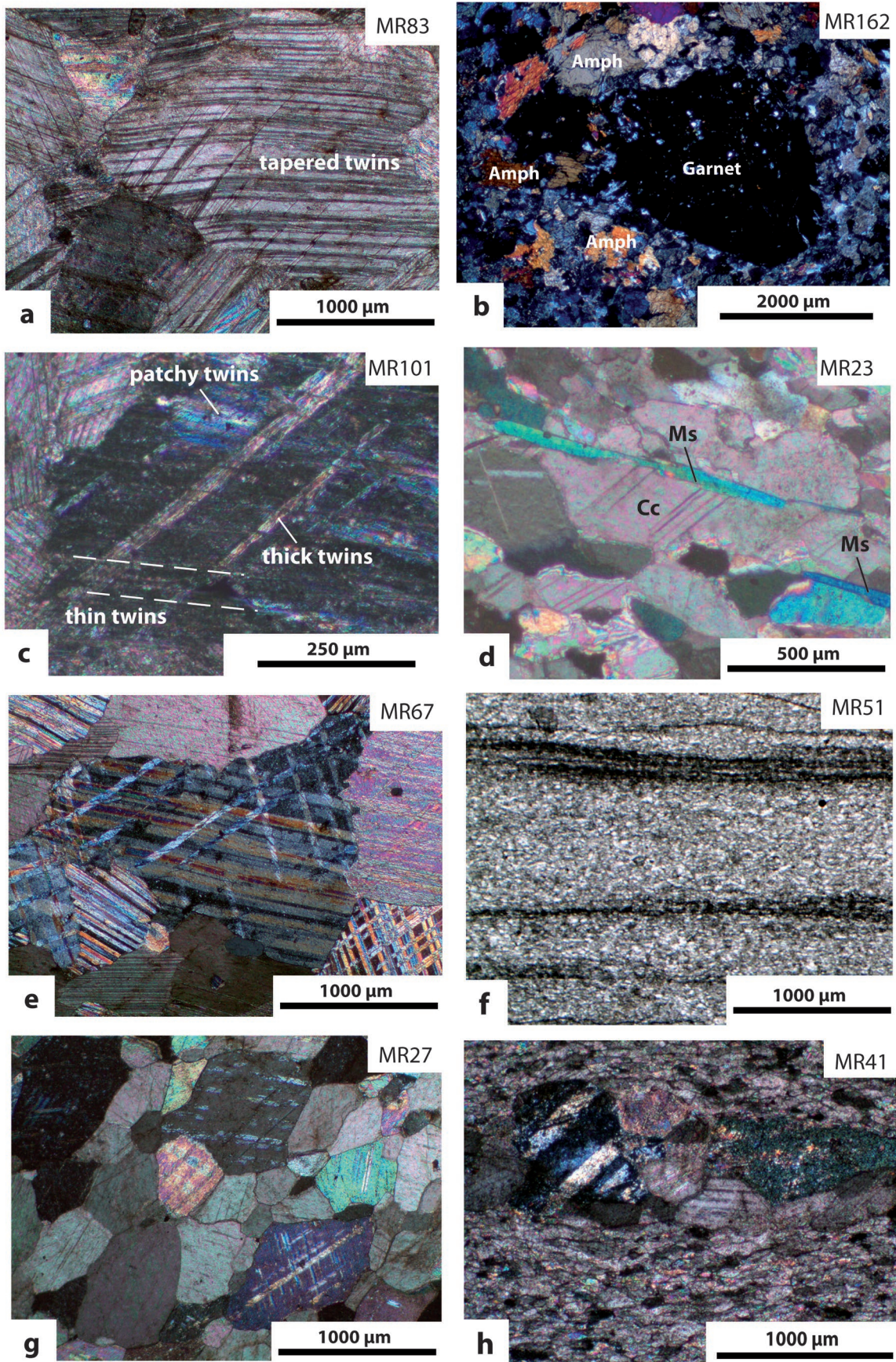
Vulturese-Belioara Series and the overthrusted Baia de Arieş Nappe. Most thin sections from samples of the Vulturese-Belioara Series (MR9, MR13, MR19, MR26, MR27, MR41) exhibit a heteroblastic texture (e.g., Fig. 6g,h and Table 1). Intermediate grain sizes of ~1–1.5 mm show well developed triple junctions and a second population of small recrystallized calcite grains around the bigger ones. Larger grains (e.g., sample MR27; Fig. 6g) exhibit patchy type IV twinning, overprinted by recrystallization and cross cut by type II and III twins (cf. scheme of Burkhard 1993). Sample MR41 from the red, platy marbles shows very small, recrystallized grains and larger ~1mm-sized calcite grains with patchy type IV twins.

$\delta^{18}O$ and $\delta^{13}C$ isotopy

Analytical data from isotope analyses (Table 2) are summarized in Fig. 7 and compared with data from Pană (1998; Table 3). Although only local names are given, the dataset from Pană (1998) allows for a general comparison with new data from this study. The studied samples cover a broad range of $\delta^{18}O$ values but cluster around 20–25 ‰ (SMOW), typical of diagenetically altered limestones (Sharp 2007). Typical greenschist-facies limestones range from –0.3 to +5.6 for carbon isotope values and from 18.1 to 28.1 for oxygen isotope values (Dunn & Valley 1985). However, the isotopic values (Fig. 7) show an interesting correlation: isolated marble lenses predominantly yield $\delta^{18}O_{VSMOW}$ values ≤20 ‰ and a large spread in $\delta^{13}C_{VPDB}$ values, whereas samples from marble sequences located at or close to nappe contacts cluster in a narrow range of $\delta^{13}C_{VPDB}$ values and predominantly yield $\delta^{18}O_{VSMOW}$ values of more than 20 ‰.

Due to Cretaceous metamorphism, all samples experienced a thermal overprint and were possibly exposed to alteration processes. However, the $\delta^{18}O_{VSMOW}$ values of most analysed samples range within the limits of typical unaltered marine limestones (between 22.6 and 30.9 ‰; Veizer et al. 1999), suggesting that metamorphism did not significantly alter the isotopic composition of the protolith. According to Fölling & Frimmel (2002), samples with $\delta^{18}O_{VSMOW}$ values between 20.6 and 16.4 (samples MR101, MR67, MR161) experienced slight alteration and $\delta^{18}O_{VSMOW}$≤16.4 indicates considerable alteration (sample MR23). All samples from the Vulturese-Belioara Series yield $\delta^{18}O_{VSMOW}$ values between 28.1 and 30.1 ‰ and a $\delta^{13}C_{VPDB}$ value between 2.1 and 2.6 ‰, which are typical for unaltered marine limestones (Veizer et al. 1999). The samples were taken from the white marbles and do not cover the dolomites and the red layer between the dolomite and marble successions. Sample MR19 from an isolated marble block along the fault in the Belioara valley shows slightly lower $\delta^{18}O_{VSMOW}$ and $\delta^{13}C_{VPDB}$ values, but still plots within the range of the Vulturese-Belioara Series. The presumably Mesozoic marbles from the Baia de Arieş Nappe (Vinţa and Sohodol Marbles) yield slightly lower values

Table 1: Important sample parameters based on the petrographic analysis of the thin sections. Abbreviations: L=marble lens within the crystalline basement; VID=marble sequence from the uppermost part of the Vidolm Nappe; SOH=Sohodol marbles from the Baia de Arieş Nappe; VIN=Vinţa marbles of the Baia de Arieş Nappe; VBS=Vulturese Belioara Series (Biharia Nappe s.str.).

Sample	Geographic Position Latitude	Longitude	Tectonic Unit	Lithostrat. Unit	Macroscopic Characterisation	Mineral composition	Texture	Dominant Twinning Type	Max. grain size [mm]
MR89	46°24'12.544" N	23°30'23.466" E	Vidolm Nappe	VID	layered and folded mylonite	Cc, Dol, Qz, Fsp, Ms	heteroblastic	2	0.5
MR99	46°27'42.078" N	23°32'23.781" E	Vidolm Nappe	VID	fine grained yellowish white marble	Cc, Ap, Ep, Ms	heteroblastic	2–3	0.5
MR101	46°28'03.425" N	23°32'28.572" E	Vidolm Nappe	VID	coarse grained yellowish white marble	Cc, Qz, Ap	heteroblastic	3	2.0
MR102	46°30'04.664" N	23°35'23.136" E	Vidolm Nappe	VID	coarse grained yellowish white marble	Cc, Ap, Mus, Py	heteroblastic	3	2.0
MR83	46°31'05.521" N	23°35'25.559" E	Vidolm Nappe	L	coarse grained white marble	Cc, Ms, Ap	homeoblastic	3	2.0
MR22	46°21'30.267" N	23°01'11.868" E	Baia de Aries N.	SOH	coarse grained light grey marble	Cc	heteroblastic	1	2.0
MR67	46°21'03.372" N	22°50'19.371" E	Baia de Aries N.	SOH	coarse grained light grey marble	Cc	homeoblastic	2	2.0
MR163	46°21'45.709" N	23°1'54.111" E	Baia de Aries N.	VIN	very coarse white marble	Cc	homeoblastic	4	2.5
MR23	46°24'19.178" N	23°13'04.455" E	Baia de Aries N.	L	fine to medium grained, beige dolomite marble	Cc, Dol, Qz, Ms	heteroblastic	2	1.0
MR51	46°29'15.245" N	23°22'13.576" E	Biharia N. s.str.	VBS	fine grained mylonite with dark layers	Cc, Qz, Py	homeoblastic	n.a.	0.05
MR26	46°30'23.343" N	23°26'33.964" E	Biharia N. s.str.	VBS	medium grained layered marble	Cc, Ms, Qz	heteroblastic	2	1.2
MR27	46°30'27.114" N	23°26'30.332" E	Biharia N. s.str.	VBS	medium grained layered marble	Cc, Ms, Qz	heteroblastic	2	1.2
MR9	46°29'46.972" N	23°25'53.775" E	Biharia N. s.str.	VBS	medium grained white marble	Cc	heteroblastic	2	1.2
MR13	46°27'33.207" N	23°23'51.913" E	Biharia N. s.str.	VBS	medium grained white marble	Cc, Ap	heteroblastic	2	1.5
MR19	46°27'47.404" N	23°22'29.406" E	Biharia N. s.str.	VBS	fine to medium grained white marble	Cc, Qz, Ser, Py	heteroblastic	2	1.2
MR41	46°30'34.50" N	23°2'619.42" E	Biharia N. s.str.	VBS	red weathered, platy marble	Cc	heteroblastic	n.a./4	1.0
MR161	46°31'49.002" N	23°34'31.059" E	Biharia N. s.str.	L	yellowish dolomite breccia	Cc, Dol	heteroblastic	3	0.4

Table 2: Overview of the results from δ ^{18}O and δ ^{13}C isotope analyses. Type refers to the lithology type: D for dolomite or C for calcite. Abbreviations: L = marble lens within the crystalline basement; VID = marble sequence from the uppermost part of the Vidolm Nappe; SOH = Sohodol marbles from the Baia de Arieş Nappe; VIN = Vinţa marbles of the Baia de Arieş Nappe; VBS = Vulturese Belioara Series (Biharia Nappe s.str.).

Sample	Geographic position		Tectonic Unit	Lithostrat. Unit	Type	C–isotopes VPDB	O–isotopes VSMOW	O–isotopes VPDB
	Latitude	Longitude						
MR89	46°24'12.544" N	23°30'23.466" E	Vidolm Nappe	VID	C	2.23	27.53	−3.28
MR99	46°27'42.078" N	23°32'23.781" E	Vidolm Nappe	VID	C	3.19	26.45	−4.32
MR100	46°27'31.955" N	23°32'28.795" E	Vidolm Nappe	VID	D	2.33	25.70	−5.05
MR101	46°28'03.425" N	23°32'28.572" E	Vidolm Nappe	VID	C	1.73	20.37	−10.23
MR102	46°30'04.664" N	23°35'23.136" E	Vidolm Nappe	VID	C	2.10	22.99	−7.68
MR83	46°31'05.521" N	23°35'25.559" E	Vidolm Nappe	L	C	2.31	22.38	−8.27
MR22	46°21'30.267" N	23°01'11.868" E	Baia de Aries N.	SOH	C	2.48	23.85	−6.85
MR67	46°21'03.372" N	22°50'19.371" E	Baia de Aries N.	SOH	C	1.87	20.05	−10.53
MR163	46°21'45.709" N	23°15'54.111" E	Baia de Aries N.	VIN	C	1.62	22.67	−7.98
MR23	46°24'19.178" N	23°13'04.455" E	Baia de Aries N.	L	C	1.37	14.91	−15.52
MR14	46°27'33.207" N	23°23'51.913" E	Biharia N. s.str.	VBS	C	2.48	29.10	−1.75
MR51	46°29'15.245" N	23°22'13.576" E	Biharia N. s.str.	VBS	C	2.43	28.21	−2.62
MR26	46°30'23.343" N	23°26'33.964" E	Biharia N. s.str.	VBS	C	2.63	29.75	−1.13
MR27	46°30'27.114" N	23°26'30.332" E	Biharia N. s.str.	VBS	C	2.06	28.11	−2.72
MR9	46°29'46.972" N	23°25'53.775" E	Biharia N. s.str.	VBS	C	2.35	29.29	−1.57
MR13	46°27'33.207" N	23°23'51.913" E	Biharia N. s.str.	VBS	C	2.64	30.09	−0.8
MR19	46°27'47.404" N	23°22'29.406" E	Biharia N. s.str.	VBS	C	1.97	26.32	−4.46
MR161	46°31'49.002" N	23°34'31.059" E	Biharia N. s.str.	L	D	0.76	18.19	−12.34
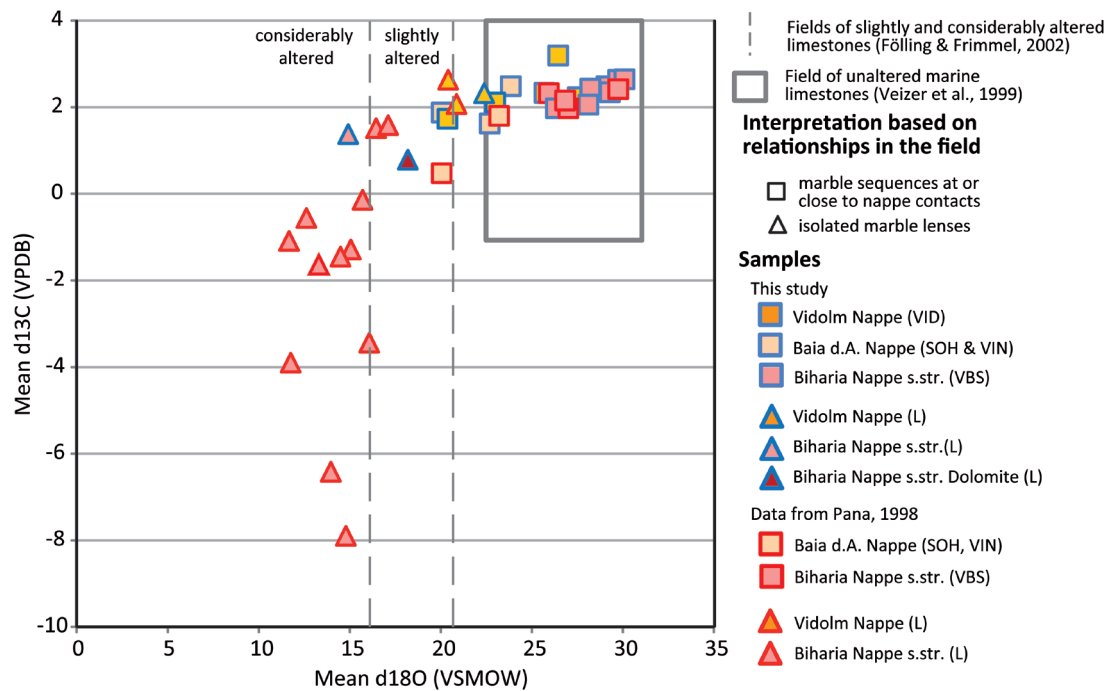
Fig. 7. Plotted results of the data from δ ^{18}O and δ ^{13}C isotope analyses. Data from the present study and data from Pană (1998) are discriminated by a red frame.

for δ ^{13}C$_{VPDB}$ (1.6–2.5 ‰) and considerably lower δ ^{18}O$_{VSMOW}$ values (20.1–23.8 ‰).

The δ ^{13}C$_{VPDB}$ values of the whole Vidolm Nappe dataset range between 1.7 and 3.2 ‰ the values of δ ^{18}O$_{VSMOW}$ range between 20.4 and 27.5 ‰. The presumably Palaeozoic marble lens from the crystalline basement of the Vidolm Nappe (sample MR83; yellow triangle with red rim in Fig. 7) also yields stable isotope values compatible with only slightly altered marbles.

Table 3: Overview of the results of δ ^{18}O and δ ^{13}C isotope analyses by Pană (1998). Type refers to the lithology type: D for dolomite or C for calcite. Abbreviations: L=marble lens within the crystalline basement; VID=marble sequence from the uppermost part of the Vidolm Nappe; SOH=Sohodol marbles from the Baia de Arieș Nappe; VIN=Vința marbles of the Baia de Arieș Nappe; VBS=Vulturese Belioara Series (Biharia Nappe s.str.).

Sample	Tectonic Unit	Lithostrat. Unit	Locality	Type	C-isotopes VPDB	O-isotopes VSMOW	O-isotopes VPDB
13892	Biharia N. s.str.	L	Sagacea Valley	C	0.57	15.89	−14.57
13789	Biharia N. s.str.	L	Avram Iancu Village	D	−1.10	11.66	−18.67
13324	Biharia N. s.str.	L	Caselor Valley (Cimpeni)	D	1.51	16.45	−14.03
13324	Biharia N. s.str.	L	Caselor Valley (Cimpeni)	D	1.58	17.11	−13.39
11203	Biharia N. s.str.	L	Lupsei Valley S	D	−6.33	14.35	−16.06
13933	Biharia N. s.str.	L	Baisori Valley	C	−3.44	16.08	−14.39
13933	Biharia N. s.str.	L	Baisori Valley	D	−5.68	14.60	−15.80
13904	Biharia N. s.str.	L	Ocolis Valley	D	0.59	13.38	−17.00
13980	Vidolm Nappe	L or VID	Iara Valley (Surduc)	C	2.63	20.41	−10.19
9947	Vidolm Nappe	L or VID	Iara Valley (Surduc)	C	1.70	19.57	−11.00
9947	Vidolm Nappe	L or VID	Iara Valley (Surduc)	D	2.70	22.75	−7.92
11116	Baia de Aries N.	SOH	Sohodol Marble	C	1.96	23.28	−7.40
11119	Baia de Aries N.	VIN	Vinta	C	1.96	23.32	−7.36
13812	Baia de Aries N.	VIN	Cioara Valley	C	0.52	20.02	−10.56
13860	Biharia N. s.str.	VBS	Belioara Valley	C	2.33	26.01	−4.75
13863	Biharia N. s.str.	VBS	Posaga Valley	C	2.44	29.54	−1.33
13914	Biharia N. s.str.	VBS	Ocolis Valley	D	2.09	26.89	−3.90

Calcite–dolomite geothermometry

Equilibrium temperatures were calculated for four samples from the Vidolm Nappe and the Biharia Nappe s.str. (see Table 4; representative analyses are given in the Supplementary data; Table S1). All temperature estimates plot within greenschist-facies thermal conditions. Samples MR26 and MR161, both from the Biharia Nappe s.str., yield slightly higher temperatures than the Vidolm samples (~354±54 °C and 370±45 °C versus ~316±52 °C and 336±37 °C; Table 4). Samples MR100 and MR89 were both taken from the calcite marble succession in the uppermost part of the Vidolm Nappe. The thermal conditions indicate lowermost greenschist-facies metamorphism and are in agreement with their relative structural position in the Biharia Nappe System. A comparison with data from Pană (1998) turned out to be difficult, because only peak temperatures of the samples are given and not the temperature range as in the dataset of this study. A conversion using the values given in figs. 5–10 in Pană (1998) seemed to be unreliable, thus only the peak temperatures of Pană (1998) are shown in Fig. 1.

Sr-isotope stratigraphy

A total number of seven samples were prepared and analysed regarding their Sr-isotopy: four samples of fine grained white marbles of the Vulturese-Belioara Series (MR9, MR13, MR26, MR27), two samples from a presumably Mesozoic marble succession of the Vidolm Nappe (MR99 and MR102) and one coarse grained sample from a marble lens within the crystalline basement of the Baia de Arieș Nappe (MR23b). ^{87}Sr/^{86}Sr isotopic ratios are corrected for a NBS987 standard of

Table 4: Results of calcite-dolomite geothermometry. Abbreviations: L=marble lens within the crystalline basement; VID=marble sequence from the uppermost part of the Vidolm Nappe; VBS=Vulturese Belioara Series (Biharia Nappe s.str.).

Sample	Tectonic Unit	Lithostrat. Unit	Analysed Cc-Dol pairs	T [in °C]	2σ
MR89	Vidolm Nappe	VID	5	336	37
MR100	Vidolm Nappe	VID	4	316	53
MR161	Biharia N. s.str.	L	4	370	45
MR26	Biharia N. s.str.	VBS	4	354	55

0.710248 and presented in Table 5 and Fig. 8. Geochemical screening of Mn, Mg, Sr and Ca provides estimates on the degree of alteration and allows discriminating samples which are likely to yield a primary Sr-isotope composition (Table 5). Additional data on the geochemical composition is shown in the Supplementary data (Table S2). Values lower than 0.010 for Mg/Ca and lower than 0.10 for Mn/Sr are indicative for a more or less primary isotopic signal with no or only insignificant alteration (Melezhik et al. 2001; Murra et al. 2011). With the exception of MR23b, all samples show no- or only slight alteration and plot within the range of possible values for marine Sr-isotopy during the Phanerozoic (Howarth & McArthur 1997). MR23b yields an isotopic ratio of 0.709541, which is significantly higher than the rest of the samples. This elevated value can be explained by the low Sr/Rb ratio (~50; corresponding to a ^{87}Rb/^{86}Sr ratio of ~0.06; see Table 5), and the contribution of radiogenic ^{87}Sr due to the decay of ^{87}Rb. Sr/Rb ratios of the other samples is >100 (corresponding to ^{87}Rb/^{86}Sr ratios of about 0.02) and the ^{87}Sr/^{86}Sr ratios range between 0.708449 and 0.707655. Generally, the primary

Table 5: Results of Sr-isotope measurements corrected for a standard value of 0.710248 for the NBS987 (see text). Abbreviations: L=marble lens within the crystalline basement; VID=marble sequence from the uppermost part of the Vidolm Nappe; VBS=Vulturese Belioara Series (Biharia Nappe s.str.). Analyses marked with an asterisk (Mn values) are at or below the limit of detection. Alteration is estimated according to the criteria of Melezhik et al. (2001).

| Sample	Tectonic Unit	Lithostr. Unit	⁸⁷Sr/⁸⁶Sr measured	±1Sigma	⁸⁷Sr/⁸⁶Sr cor(0.710248)	± 2Sigma cor(0.710248)	Rb [ppm]	Sr [ppm]	Ca wt. %	Mg wt. %	Mn [ppm]	Mg/Ca	Mn/Sr	Alteration
MR9	Biharia N. s.str.	VBS	0.707948	0.000004	0.707950	0.000008	1	163	39.0869	0.2774	7.7*	0.007	0.05	no
MR13	Biharia N. s.str.	VBS	0.707653	0.000005	0.707655	0.000009	1	167	39.0655	0.3076	7.7*	0.008	0.05	no
MR23	Biharia N. s.str.	L	0.709539	0.000004	0.709541	0.000008	2	99	20.5619	10.1803	69.7	0.500	0.70	–
MR26	Biharia N. s.str.	VBS	0.707681	0.000004	0.707677	0.000008	1	184	38.3008	0.5549	7.7*	0.014	0.04	little
MR27	Biharia N. s.str.	VBS	0.708038	0.000004	0.708034	0.000008	1	153	38.5080	0.3679	7.7*	0.010	0.05	little
MR99	Vidolm Nappe	VID	0.708326	0.000004	0.708296	0.000007	1	244	38.4437	0.2412	7.7*	0.006	0.03	no
MR102	Vidolm Nappe	VID	0.708479	0.000003	0.708449	0.000007	1	207	38.1578	0.2231	15.5	0.006	0.07	no

*at or below detection limit
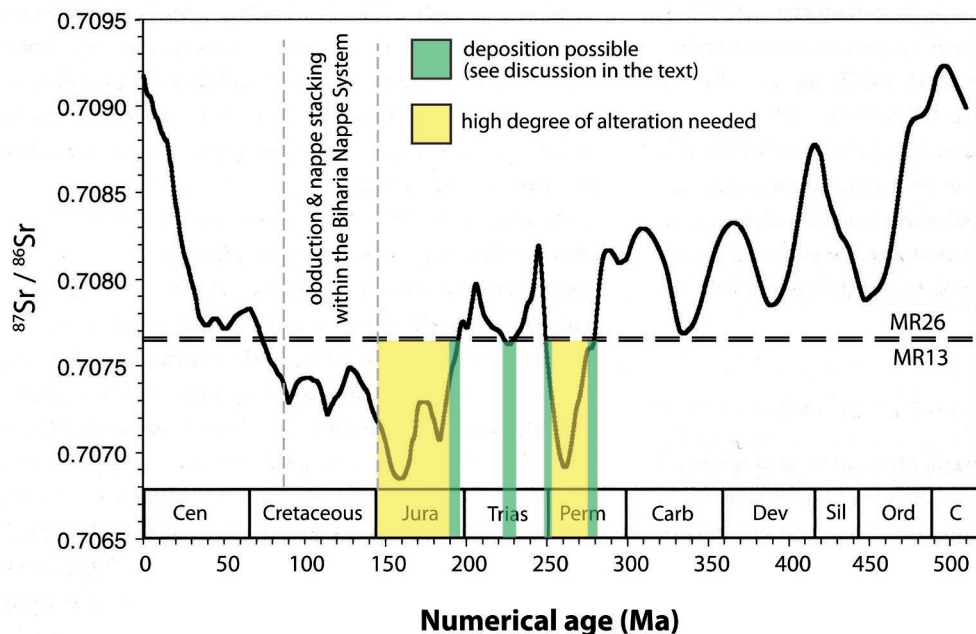
Fig. 8. Plotted ⁸⁶Sr/⁸⁷Sr ratios (horizontal lines) of samples MR13 and MR26 which intersected with the variation of ⁸⁶Sr/⁸⁷Sr through the Phanerozoic time modified from McArthur et al. (2004). Samples MR26 and MR13 from the Vulturese-Belioara Series were selected as they provide a low Sr-ratio which allows for a meaningful discrimination of depositional intervals. The Cretaceous interval is excluded due to intense nappe stacking and metamorphic overprinting of the Biharia Nappe System.

^{87}Sr/^{86}Sr isotopic ratio of marine carbonate rocks situated within the continental crust can only increase to higher values due to post-depositional alteration during diagenesis and metamorphism (Brand & Veizer 1980, 1981). Consequently, the lowest ^{87}Sr/^{86}Sr ratios of MR26 (0.707677) and MR13 (0.707655) have been accepted as the best proxy for the sea-water composition (Table 5 and Fig. 8) and allow narrowing down of the range of possible sedimentation periods. While the Mg/Ca ratio of sample MR26 (0.014) indicates little alteration, the ratio of MR13 (0.008) indicates a primary signal. Low Mn/Sr ratios of 0.04 for sample MR26 and 0.05 for sample MR13 also point to a primary signature with very little alteration (e.g., Jacobsen & Kaufman 1999; Melezhik et al. 2001; Fölling & Frimmel 2002). Higher ^{87}Sr/^{86}Sr ratios (see

other samples) yield a high number of intercepts with the marine Sr-isotope curve and thus inhibit further interpretation.

Discussion

Biharia Nappe s.str.

Stratigraphic correlation of the Vulturese Belioara Series

The clastic meta-sediments (meta-sandstones, quartzitic conglomerates and sericitic schists) at the base of the Vulturese-Belioara series (Figs. 3b, 5) show similarities to other Permian to Lower Triassic deposits of the Circum-Pannonian

region (Burchfiel 1976; Vozárová et al. 2010; Kovács et al. 2010). Ianovici et al. 1976, correlate the red, laminated meta-conglomerates of the Biharia Nappe with Permian deposits of the Codru Nappe System. Balintoni et al. (2002) also discuss the occurrence of red, Permian meta-conglomerates in both, the Biharia and Codru nappe systems.

In the Anisian, dark grey dolomites are documented for the Bucovinian, the Transilvanides, the Pădurea Craiului (Bihor Unit) the Arieşeni Nappe (Biharia Nappe System) and several nappes of the Codru Nappe System (e.g., Finiş-Gîrda Nappe; Patrulius et al. 1971; Burchfiel & Bleahu 1976; Vörös 2000; Kovács et al. 2010). Together with the presence of crinoids (pers. comm. Emanoil Sasaran and field observations by Trümpy in Balintoni 1994a) we infer a Middle Triassic (Anisian) depositional age for the black and grey dolomites. Increasing thickness of the dolomites towards the NE, possibly relates to variations in the primary thickness of the dolomites or to tectonic omission (compare Fig. 2 and Fig. 5). During the Triassic, the Tisza and Dacia Mega-units were situated in neighbouring positions on the European continental margin (e.g., Săndulescu 1984; Vörös 1993; Csontos & Vörös 2004; Haas & Péró 2004; Schmid et al. 2008) and thus allow for a correlation between the Permo–Mesozoic sediments of their nappe systems. Ianovici et al. (1976) already published correlations between the Bucovinian Nappes, Transylvanian Nappes and Codru Nappe System. Following the aforementioned model and using the distribution of Lower Triassic–Liassic facies zones, Kovács (1982) correlated the Arieşeni Nappe (Biharia Nappe System; Balintoni et al. 2002, Balintoni & Puşte 2002) with the Finiş Nappe (Codru Nappe System). However, due to intense facies differentiation from Anisian times onwards, a correlation between the Triassic sediments of the aforementioned units is difficult to undertake (c.f. Burchfiel & Bleahu 1976; Vörös 2000). The thin layer (0.5–5 m; Fig. 3c) of red, sericite-rich, platy marbles which separates grey to reddish dolomites and white marbles could correspond to red, condensed limestones of Upper Triassic (possibly Carnian?) age. All $\delta^{18}O$ and $\delta^{13}C$ values from the Vulturese-Belioara Series plot within the field of unaltered marine marbles (according to Veizer et al. 1999). $\delta^{18}O$ and $\delta^{13}C$ isotopy also allows for a clear distinction between the Vulturese-Belioara Series and calcite/dolomite marble lenses from structurally lower parts of the Biharia Nappe s.str. (Fig. 7). The studied samples from the VBS show mostly homogeneous distributions of C, O and Sr isotope ratios, which do not suggest obvious post-depositional alteration. This is supported by the high $\delta^{18}O$ values, which are commonly more sensitive to post-depositional resetting than the carbon isotope system. Intersecting the results of Sr-isotope analyses with the marine Sr-isotope curve (Table 5 and Fig. 8) allows for the discrimination of several possible deposition intervals for the light calcite marbles of the Vulturese-Belioara Series.

Using the lowest $^{87}Sr/^{86}Sr$-values from MR13 and MR26, the Silurian, Devonian and Carboniferous intervals can be excluded and three intervals for deposition during the Permian, Triassic and Jurassic/Cretaceous remain (Fig. 8). The Permian

interval can also be virtually excluded since no comparable carbonate sequences (consisting of quartzite conglomerates, dolomite and calcite marbles) are present in the Circum-Pannonian realm during this time span (cf. Seghedi et al. 2001; Vozárová et al. 2010). Furthermore, the clastic meta-sediments at the base of the sequence are already interpreted as Permo–Triassic deposits (see text above). It is possible to conclude that the results of Sr-isotope analyses support the interpretation of the Vulturese-Belioara Series as Mesozoic cover of the Biharia Nappe s.str. Possible age intervals for deposition of the light grey calcite marbles are 231–220 Ma (Ladinian to Carnian), and 195–72 Ma (Jurassic and Cretaceous). Given that the Biharia Nappe System experienced Late Jurassic emplacement of the South Apuseni Ophiolites (e.g., Csontos et al. 2002; Schmid et al. 2008; Kounov & Schmid 2013; Gallhofer et al. 2016), followed by deformation and metamorphism during the Early Cretaceous, the Jurassic–Cretaceous interval can be further restricted to 145–195 Ma. Assuming a primary isotopic signal with no or only a little alteration (Fig. 7 and Table 5) for the samples MR13 and MR26 a Mid Triassic or Early Jurassic deposition of the light grey calcite marbles is indicated. Thus, depending on the interpretation of the red, condensed marbles as possible Carnian deposits, a Jurassic deposition of the overlying grey marbles has to be favoured.

Thermotectonic evolution

Based on calcite–dolomite geothermometry, the thermal overprint can be constrained to 354±55 °C in the light grey marbles of the Vulturese-Belioara Series (sample MR26; Table 4). Marble lenses in the structurally lower parts of the Biharia Nappe s.str. show slightly higher thermal conditions (370±45 °C see sample MR161 and data by Pană 1998). Late Cretaceous zircon fission track ages (82–89 Ma; Kounov & Schmid 2013) allow constraining of the thermal conditions during the Late Cretaceous to ≤300 °C (cf. Reiser et al. 2016). Whereas Ar–Ar muscovite data (113 Ma; Reiser et al. 2016) from the basement in the footwall of the Vulturese-Belioara Series indicate thermal conditions around 425° C (Harrison et al. 2009) during Early Cretaceous times. Thus, the overprint of the Vulturese-Belioara Series, as indicated by calcite–dolomite geothermometry (~350 °C), can be constrained to late Early Cretaceous or mid Cretaceous times (NW-directed nappe stacking during D2; sensu Reiser et al. 2016). Recrystallization processes visible in the thin sections presumably relate to this thermal imprint (see Fig. 6f). NE–SW trending fold axes and SE-dipping bedding planes from the Vulturese-Belioara Series also correlate with NW-directed thrusting and nappe stacking during D2 (e.g., Ianovici et al. 1976; Balintoni et al. 1996). Thin type I twins which form at temperatures ≤200 °C (Burkhard 1993), together with brittle deformation and apatite fission track data around 60 Ma (Sanders 1998; Merten et al. 2011; Kounov & Schmid 2013) constrain the late Maastrichtian–middle Eocene (D4) thermal imprint.

Baia de Arieş Nappe

Although the quartzitic conglomerates and sericitic schists at the base of the Sohodol marble sequence resemble typical Permo–Early Triassic sequences, our dataset does not allow for a meaningful interpretation as a Mesozoic sequence (as proposed by Ianovici et al. 1976). However, the O and C isotopic values which plot within the frame of greenschist-facies altered marbles do not inhibit this interpretation (Fig. 7). The presence of several different types of twinning in the thin sections allows us to infer a polyphase deformation of the Sohodol Marbles with the last stage at low temperatures, less than 200 °C (Passchier & Trouw 1996; Ferrill et al. 2004). The presence of Late Cretaceous post-tectonic sediments (Schuller 2004; Schuller et al. 2009) overlying the marbles indicate thermal conditions for the Sohodol Marbles of ≤200 °C during Late Cretaceous times.

Vidolm Nappe

The isotopic values of marble lenses within the Vidolm basement are close to the values of the Mesozoic cover, the structural position (Fig. 1) and the presence of eclogitic bodies associated with the marbles indicate a Palaeozoic origin. Pană (1998) reported thermal conditions of about 500 °C (Cc–Dol thermometry) from the aforementioned marbles. It follows that their isotopic composition did not significantly change, even under high-grade conditions. Furthermore, the Sr-ratios of the marbles from the top of the Vidolm Nappe (Fig. 8) turned out to be too high to allow for a meaningful distinction between a Palaeozoic and Mesozoic deposition age and thus are not considered for further interpretation. The attribution of a depositional age to the other dolomite and calcite marbles is difficult. However, the clastic sequence at the base of the marbles allows for a tentative correlation with the Vulturese-Belioara Series (Fig. 9). The results of calcite–dolomite geothermometry provide evidence for a greenschist-facies overprint (reaching temperatures of ~320 °C; Fig. 4) of the calcite and dolomite marbles at the top of the Vidolm Nappe. Since samples from the Vidolm basement already cooled below the zircon partial annealing zone (PAZ) at about 100 Ma (Kounov & Schmid 2013), the thermal imprint recorded by the samples MR89 and MR100 occurred during Early Cretaceous times, namely during an early stage of D2 or already during D1 (sensu Reiser et al. 2016; i.e. presumably E- or NE-directed deformation following the obduction of the South Apuseni Ophiolites).

Conclusions

The new isotopic and geochemical dataset in combination with field observations on the stratigraphic sequences and the correlation with Mesozoic sequences in the Circum-Pannonian region allow for an attribution of the siliciclastic and carbonatic lithologies of the Vulturese-Belioara Series to different depositional periods during the Permo–Mesozoic interval. Sr-isotope analyses from pure white marbles of the Vulturese-Belioara Series provide evidence for a Middle/Late Triassic or a Jurassic deposition. However, the results of this study can only provide basic information on the depositional age of the Vulturese Belioara Series. In order to provide a detailed stratigraphy, a larger number of samples has to be analysed. The Biharia Nappe s.str. experienced greenschist-facies metamorphic overprint and large-scale folding of the Vulturese-Belioara Series around NE-SW trending fold axes during late Early/early Late Cretaceous, top-NW directed nappe stacking (D2). The results from other marble sequences (Vidolm and Baia de Arieş nappes) do not allow for a clear
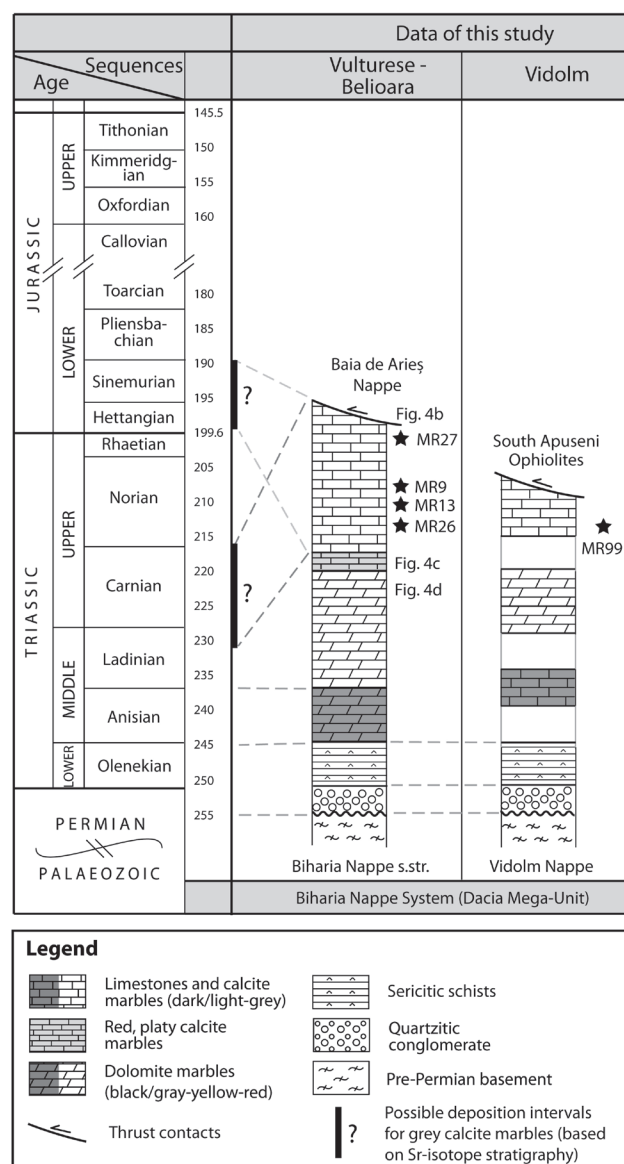

Fig. 9. Stratigraphic columns to allow for a tentative correlation of the sedimentary sequences of the Biharia Nappe System. Dashed lines indicate tentative correlations between the lithostratigraphic units. For the Vidolm occurrences, only the relative succession is given in the figure.

attribution; however the new data might provide helpful information for future studies. Correlating the thermal data from the marble sequences with the tectonothermal evolution of the Apuseni Mountains constrains greenschist-facies conditions during the Alpine event in late Early/early Late Cretaceous times.

References

Anovitz L.M. & Essene E. 1987: Phase equilibria in the system $CaCO_3$–$MgCO_3$–$FeCO_3$. *J. Petrol.* 28, 389–415.

Balintoni I. 1994a: Some new data about the Structure of the Apuseni Mountains. *Studia Univ. Babeş-Bolyai, Geologia* 39, 1–2.

Balintoni I. 1994b: Structure of the Apuseni Mts. ALCAPA II. Field Trip Guidebook. *Rom. J. Tecton. Reg. Geol.* 75, 51–58.

Balintoni I. & Iancu V. 1986: Lithostratigraphic and tectonic units in the Trascău Mountains, north of Mânăstirea Valley. *DS Ins. Geol. Geofz.* 70–71, 45–56.

Balintoni I. & Vlad C. 1996: Tertiary magmatism in the Apuseni Mountains and related tectonic setting. *Studia Univ. Babeş-Bolyai, Geologia* 41, 115–126.

Balintoni I. & Puşte A. 2002: New lithostratigraphic and structural aspects in the southern part of the Bihor Massif (Apuseni Mountains). *Studia Univ. Babeş-Bolyai, Geologia* 47, 13–18.

Balintoni I., Lupu M., Iancu V. & Lazăr C. 1987: Geological map of Romania, scale 1:50,000; sheet Poşaga. *Inst. Geol. Geof.*, Bucureşti (in Romanian).

Balintoni I., Puşte A. & Stan R. 1996: The Codru nappe system and the Biharia Nappe System: A comparative argumentation. *Studia Univ. Babeş-Bolyai, Geologia* 41, 101–113.

Balintoni I., Ghergari L. & Băbuţ T. 2002: The Arieseni Nappe, or the Moma and Poiana Nappes?. *Studia Univ. Babeş-Bolyai, Geologia* 47, 2, 19–26.

Balintoni I., Balica C., Cliveti M., Li L.Q., Hann H.P., Chen F.K. & Schuller V. 2009: The emplacement age of the Muntele Mare Variscan granite (Apuseni Mountains, Romania). *Geol. Carpath.* 60, 95–504.

Balintoni I., Balica C., Ducea M.N., Zaharia L., Chen F.K., Cliveti M., Hann H.P., Li L.Q. & Ghergari L. 2010: Late Cambrian–Ordovician northeastern Gondwanan terranes in the basement of the Apuseni Mountains, Romania. *J. Geol. Soc.* 167, 1131–1145.

Bleahu M., Lupu M., Patrulius D., Bordea S., Stefan A. & Panin S. 1981: The structure of the Apuseni Mountains. In: XII Congress (Bucharest, Romania). Guide to Excursion-B3, Carpatho-Balkan Geological Association. *Institute Of Geology and Geophysics,*

Bucharest, 103.

Bordea S., Dimitrescu R., Mantea G., Stefan A., Bordea J., Bleahu M. & Costea C. 1988: Geological map of Romania, scale 1:50,000; sheet Biharia. *Inst. Geol. Geof.*, Bucureşti (in Romanian) .

Brand U. & Veizer J. 1980: Chemical diagenesis of a multicomponent carbonate system-1: Trace elements. *J. Sediment. Res.* 50, 1219–1236.

Brand U. & Veizer J. 1981: Chemical diagenesis of a multicomponent carbonate system-2: Stable isotopes. *J. Sediment. Res.* 51, 987–997.

Burchfiel B.C. & Bleahu M. 1976: Geology of Romania. *Geol. Soc. Am. Spec. Pap.* 158, 1–82.

Burkhard M. 1993: Calcite twins, their geometry, appearance and significance as stress-strain markers and indicators of tectonic regime: a review. *J. Struct. Geol.* 15, 351–368.

Csontos L., Benkovics L., Bergerat F., Mansy J.L. & Wórum G. 2002: Tertiary deformation history from seismic section study and fault analysis in a former European Tethyan margin (the Mecsek-Villány area, SW Hungary). *Tectonophysics* 357, 81–102.

Csontos L. & Vörös A. 2004: Mesozoic plate tectonic reconstruction of the Carpathian region. *Palaeogeogr. Palaeoclimatol. Palaeoecol.* 210, 1–56.

Dallmeyer R.D., Pană D.I., Neubauer F. & Erdmer P. 1999: Tectonothermal evolution of the Apuseni Mountains, Romania: Resolution of Variscan versus Alpine events with 40Ar/39Ar ages. *J. Geol.* 107, 329–352.

Dunn S. & Valley J. 1985: Fluid infiltration of the Tudor gabbro during regional metamorphism. *Geol. Soc. Am. Abstr. Prog.* 17, 570.

Essene E.J. 1983: Solid solutions and solvi among metamorphic carbonates with applications to geologic thermobarometry. *Rev. Mineral. Geochem.* 11, 77–96.

Ferrill D.A. 1991: Calcite twin widths and intensities as metamorphic indicators in natural low-temperature deformation of limestone. *J. Struct. Geol.* 13, 667–675.

Ferrill D.A., Morris A.P., Evans M.A., Burkhard M., Groshong Jr. R.H. & Onasch C.M. 2004: Calcite twin morphology: a low-temperature deformation geothermometer. *J. Struct. Geol.* 26, 1521–1529.

Fölling P. & Frimmel H. 2002: Chemostratigraphic correlation of carbonate successions in the Gariep and Saldania Belts, Namibia and South Africa. *Basin Res.* 14, 69–88.

Frank W., Hammer St., Popp F., Scharbert S. & Thöni M. 1990: Isotopengeologische Neuergebnisse zur Entwicklungsgeschichte der Böhmischen Masse: Proterozoische Gesteinsserien und Variszische Hauptorogenese. *Publikation Zentralanstalt für Meteorologie und Geodynamik* 1990/3, 185–228.

Gallhofer D., von Quadt A., Schmid S.M., Guillong M., Peytcheva I. & Seghedi I. 2016: Magmatic and tectonic history of Jurassic ophiolites and associated granitoids from the South Apuseni Mountains (Romania). *Swiss J. Geosci.* doi: 10.1007/s00015-016-0231-6

Haas J., Kovács S., Karamata S., Sudar M., Gawlick H.J., Grădinaru E., Mello J., Polák M., Péró C., Ogorelec B. & Buser S. 2010: Jurassic environments in the Circum-Pannonian region. In: Vozár J., Ebner F., Vozárová A., Haas J., Kovács S., Sudar M., Bielik M., Péró C. (Eds.): Variscan and Alpine terranes of the Circum-Pannonian Region. *Geol. Inst. SAS*, Bratislava, Chapter 5, 157–202.

Haas J. & Péró C. 2004: Mesozoic evolution of the Tisza Mega-Unit. *Int. J. Earth Sci.* 93, 297–313.

Howarth R. & McArthur J. 1997: Statistics for strontium isotope stratigraphy: a robust LOWESS fit to the marine Sr-isotope curve for 0 to 206 Ma, with look-up table for derivation of numeric age (look-up table version 4: 08/03). *J. Geol.* 105, 441–456.

Ianovici V., Borcoş M., Bleahu M., Patrulius D., Lupu M., Dimitrescu

R. & Savu H. 1976: Geology of the Apuseni Mountains. *Acad. R.S.R.*, Bucureşti, 1–631.

Ilie M. 1936. Recherches geologiques dans les Monts Trascău et dans le bassin de l'Aries. *AIGR,* Bucureşti, XVII, 329–466.

Jacobsen S.B. & Kaufman A.J. 1999: The Sr, C and O isotopic evolution of Neoproterozoic seawater. *Chem. Geol.* 161, 37–57.

Jamison W.R. & Spang J.H. 1976: Use of calcite twin lamellae to infer differential stress. *Geol. Soc. Am. Bull.* 87, 868–872.

Kounov A. & Schmid S. 2013: Fission-track constraints on the thermal and tectonic evolution of the Apuseni Mountains (Romania). *Int. J. Earth Sci.* 102, 207–233.

Kovács S. 1982: Problems of the „Pannonian Median Massif "and the plate tectonic concept. Contributions based on the distribution of Late Paleozoic—Early Mesozoic isopic zones. *Geol. Rundsch.* 71, 2, 617–639.

Kovács S., Sudar M., Karamata S., Haas J., Péró C., Grădinaru E., Gawlick H.J., Gaetani M., Mello J., Polák M., Aljinović D., Ogorelec B., Kolar-Jurkovšek T., Jurkovšek B. & Buser S. 2010: Triassic environments in the Circum-Pannonian region related to the initial Neotethyan rifting stage. In: Vozár J., Ebner F., Vozárová A., Haas J., Kovács S., Sudar M., Bielik M., Péró C. (Eds.): Variscan and Alpine terranes of the Circum-Pannonian Region. *Geol. Inst. SAS*, Bratislava, Chapter 4, 87–156.

Kräutner H. 1980: Lithostratigraphic Correlation of Precambrian In The Romanian Carpathians. *Annu. Inst. Geol. Geog.* 57, 229–296.

Krézsek C. & Bally A.W. 2006: The Transylvanian Basin (Romania) and its relation to the Carpathian fold and thrust belt: Insights in gravitational salt tectonics. *Mar. Petrol. Geol.* 23, 405–442.

Kutassy A. 1928a: Die Ausbildung der Trias in Moma-Gebirge (Ungarn-Siebenbürgen). *Centralbl. F. Min. Geol. U. Pal.*, Abt. B, 320–325.

Kutassy A. 1928b: Die Triasschichten des Bêler und Bihargebirges (Siebenbürgen, Ungarn) mit besonderer Rücksicht auf die stratigraphische Lage ihres Rhätikums. *Verh. Geol. Bundesanst.* Wien.

Letargo C.M., Lamb W.M. & Park J.S. 1995: Comparison of calcite+dolomite thermometry and carbonate+silicate equilibria: Constraints on the conditions of metamorphism of the Llano uplift, central Texas, USA. *Am. Mineral.* 80, 131–143.

Lupu M. 1972: Stratigraphy and structure of the Mesozoic formations in the Trascău Mountains. *Summary of PhD thesis, University of Bucharest*, 1–56 (in Romanian).

Mârza I. 1965: Petrographic and palaeostratigraphic units of metamorphic carbonate massifs: Vulturese-Scărisoara-Leurda (Arieş Basin). *Analele Universităţii Bucureşti: Seria ştiinţele naturii. Geologie-Geografie* 14, 9–17 (in Romanian).

Mârza I. 1969: Evolution of the crystalline units southeast of the Muntele Mare. *Ed. Acad. Rom.*, Bucharest, 1–168 (in Romanian).

McArthur J. 1994: Recent trends in strontium isotope stratigraphy. *Terra Nova* 6, 331–358.

McArthur J., Howarth R. & Bailey T. 2001: Strontium isotope stratigraphy: LOWESS version 3: best fit to the marine Sr-isotope curve for 0–509 Ma and accompanying look-up table for deriving numerical age. *J. Geol.* 109, 155–170.

McArthur J., Mutterlose J., Price G., Rawson P., Ruffell A. & Thirlwall M. 2004: Belemnites of Valanginian, Hauterivian and Barremian age: Sr-isotope stratigraphy, composition ($^{87}Sr/^{86}Sr$, $\delta 13C$, $\delta 18O$, Na, Sr, Mg), and palaeo-oceanography. *Palaeogeogr. Palaeoclimatol. Palaeoecol.* 202, 253–272.

McArthur J., Howarth R. & Shields G. 2012: Strontium isotope stratigraphy. *A geologic time scale*, 127–144.

Melezhik V., Gorokhov I., Fallick A. & Gjelle S. 2001: Strontium and carbon isotope geochemistry applied to dating of carbonate sedimentation: an example from high-grade rocks of the Norwegian Caledonides. *Precambrian Res.* 108, 267–292.

Melezhik V.A., Roberts D., Gjelle S., Solli A., Fallick A.E., Kuznetsov A.B. & Gorokhov I.M. 2013: Isotope chemostratigraphy of high-grade marbles in the Rognan area, North-Central Norwegian Caledonides: a new geological map, and tectonostratigraphic and palaeogeographic implications. *Nor. J. Geol.* 93, 107–139.

Merten S., Matenco L., Foeken J.P.T. & Andriessen P.A.M. 2011: Toward understanding the post-collisional evolution of an orogen influenced by convergence at adjacent plate margins: Late Cretaceous–Tertiary thermotectonic history of the Apuseni Mountains. Tectonics 30, TC6008.

Murra J.A., Baldo E.G., Galindo C., Casquet C., Pankhurst R.J., Rapela C.W. & Dahlquist J. 2011: Sr, C and O isotope composition of marbles from the Sierra de de Ancasti, Eastern Sierras Pampeanas, Argentina: age and constraints for the Neoproterozoic–Lower Paleozoic evolution of the proto-Gondwana margin. *Geol. Acta* 9, 1, 79–92.

Panã D. 1998: Petrogenesis and tectonics of the basement rocks of the Apuseni Mountains, significance for the alpine tectonics of the Carpathian-Pannonian region. *PhD thesis. Univ. of Alberta,* 1–712.

Passchier C.W. & Trouw R.A. 1996: Microtectonics. Volume 256. *Springer*, Berlin, 1–289.

Patrulius D., Bleahu M., Popescu E. & Bordea S. 1971: The Triassic Formation of the Apuseni Mountains and the East Carpathians Bend. *Guidebook to excursions* 8, 1–86.

Reiser M.K. 2015: The tectonometamorphic evolution of the Apuseni Mountains during the Cretaceous. *Ph.D. thesis. University of Innsbruck*, 1–156.

Reiser M.K., Schuster R., Spikings R., Tropper P. & Fügenschuh B. 2016: From nappe stacking to exhumation: Cretaceous tectonics in the Apuseni Mountains (Romania). *Int J. Earth Sci. (Geol. Rundsch.)*, doi:10.1007/s00531-016-1335-y

Sanders C.A.E. 1998: Tectonics and Erosion, Competitive forces in a compressive orogen. A fission track study of the Romanian Carpathians. *Published PhD thesis. Vrije Universiteits*, Amsterdam, 1–204.

Savu H. 2007: Genesis of Mureş ophiolitic suture and of its N-type MORB rocks and island arc volcano-plutonic association. *Proc. Rom. Acad.*, Series B 1, 23–32.

Satish-Kumar M., Miyamoto T., Hermann J., Kagami H., Osanai Y. & Motoyoshi Y. 2008: Pre-metamorphic carbon, oxygen and strontium isotope signature of high-grade marbles from the Lützow-Holm Complex, East Antarctica: apparent age constraints of carbonate deposition. In: Satish-Kumar M., Motoyoshi Y., Osanai Y., Hiroi Y. and Shiraishi K. (Eds.): Geodynamic evolution of East Antarctica: a key to the East–West Gondwana connection. *Geol. Soc. London, Spec. Publ.* 308, 147–164.

Schmid S.M., Bernoulli D., Fügenschuh B., Matenco L., Schefer S., Schuster R., Tischler M. & Ustaszewski K. 2008: The Alpine-Carpathian-Dinaridic orogenic system: correlation and evolution of tectonic units. *Swiss J. Geosci.* 101, 139–183.

Schuller V. 2004: Evolution and geodynamic significance of the Upper Cretaceous Gosau basin in the Apuseni Mountains (Romania). *Tübinger Geowiss. Arb.,* Reihe A70, 1–112.

Schuller V. & Frisch W. 2006: Heavy mineral provenance and paleocurrent data of the Upper Cretaceous Gosau succession of the Apuseni Mountains (Romania). *Geol. Carpath.* 57, 29–39.

Schuller V., Frisch W., Danisik M., Dunkl I. & Melinte M.C. 2009: Upper Cretaceous Gosau Deposits of the Apuseni Mountains (Romania) — Similarities and differences to the Eastern Alps. *Austrian J. Earth Sci.* 102, 133–145.

Seghedi A., Popa M., Oaie G. & Nicolae I. 2001: The Permian system in Romania. Permian continental deposits of Europe and other areas. *Regional reports and correlations*, Brescia, 281–293.

Sharp Z. 2007: Principles of stable isotope geochemistry. *Pearson education Upper Saddle River*, NJ, 1–344.

Solomon I., Moţoi G., Moţoi A., Mărgărit M. & Mărgărit G. 1981: Geological investigations on the eastern flank of the Gilău Mountains (Apuseni Mountains). *D.S. Inst. Geol. Geofz.* 68, 115–139 (in Romanian).

Sölva H., Grasemann B., Thöni M., Thiede R. & Habler G. 2005: The Schneeberg normal fault zone: Normal faulting associated with Cretaceous SE-directed extrusion in the eastern Alps (Italy/Austria). *Tectonophysics* 401, 143–166.

Spötl C. & Vennemann T.W. 2003: Continuous-flow isotope ratio mass spectrometric analysis of carbonate minerals. *Rapid communications in mass spectrometry* 17, 1004–1006.

Săndulescu M. 1984: Geotectonics of Romaniâ. *Editura Tehnică Bucharest*, 1–366 (in Romanian).

Săsăran E. 2005: Upper Jurassic–Lower Cretaceous carbonates sedimentation from Bedeleu nappe (Apuseni Mountains): Facies, biostratigraphy and sedimentary evolution. *PhD thesis. Babes-Bolyai University,* Cluj-Napoca, 1–317 (in Romanian).

Veizer J., Ala D., Azmy K., Bruckschen P., Buhl D., Bruhn F., Carden G., Diener A., Ebneth S. & Godderis Y. et al. 1999: [87]Sr/[86]Sr, δ^{13}C and δ^{18}O evolution of Phanerozoic seawater. *Chem. Geol.* 161, 59–88.

Veizer J., Buhl D., Diener A., Ebneth S., Podlaha O., Bruckschen P., Jasper T., Korte C., Schaaf M. & Ala D. et al. 1997: Strontium isotope stratigraphy: potential resolution and event correlation. *Palaeogeogr. Palaeoclimatol. Palaeoecol*. 132, 65–77.

Vörös A. 1993: Jurassic microplate movements and brachiopod migrations in the western part of the Tethys. *Palaeogeogr. Palaeoclimatol. Palaeoecol.* 100, 125–145.

Vörös A. 2000: The Triassic of the Alps and Carpathians and its inter-regional correlation. *Developments in Palaeontology and Stratigraphy* 18, 173–196.

Vozár J., Ebner F., Vozárová A., Haas J., Kovács S., Sudar M., Bielik M. & Péró C. (Eds.) 2010: Variscan and Alpine terranes of the Circum-Pannonian Region. *Geological Institute SAS*, Bratislava, 1–233.

Vozárová A., Ebner F., Kovács S., Kräutner H.G., Szederkényi T., Krstić B., Sremac J., Aljinović D., Novak M. & Skaberne D. 2010: Late variscan (carboniferous to permian) environments in the Circum-Pannonian region. In: Vozár J., Ebner F., Vozárová A., Haas J., Kovács S., Sudar M., Bielik M., Péró C. (Eds.): Variscan and Alpine terranes of the Circum-Pannonian Region. *Geol. Inst. SAS*, Bratislava, Chapter 3, 51–86.

Supplementary data

Table S1: Representative microprobe analyses of calcite and dolomite.

Tect. Unit	Vidolm Nappe				Biharia Nappe s.str.			
Sample #	MR89		MR100		MR161		MR26	
	cc	dol	cc	dol	cc	dol	cc	dol
oxide wt %								
Na	0.0204	0.0374	0.0087	0.0279	0.0188	0.026	0.0223	0.0146
Mg	0.7792	20.33	0.8879	20.1	0.6360	20.17	0.7174	21.91
K	0.0464	0.1338	–	–	–	0.0022	0.021	0.001
Ca	56.4	30.67	56.5	33.81	53.08	28.17	55.82	29.63
Fe	0.1557	1.5	0.0608	–	0.1479	1.87	0.0179	0.0165
Si	0.0564	0.082	0.0215	0.0577	0.0616	0.0888	0.0737	0.0468
Al	–	0.0012	–	–	–	–	–	–
Cr	–	–	–	–	–	–	–	–
Ti	0.0067	0.0111	0.0043	0.007	–	0.0028	–	–
Mn	0.1041	0.0993	0.0253	–	0.004	0.4822	–	–
P	–	–	–	–	0.0172	–	–	–
Zn	–	–	–	–	0.0429	0.0224	0.1053	0.0180
O	–	–	–	–	–	–	–	–
Total	57.57	52.87	57.51	54.00	54.01	50.84	56.78	51.64
formula calculation based on 1 oxygen								
Na	0.0063	0.0011	0.0003	0.0008	0.0006	0.0008	0.0007	0.0004
Mg	0.0187	0.467	0.0213	0.4515	0.0163	0.481	0.0175	0.506
K	0.0009	0.0026	–	–	–	–	0.0004	–
Ca	0.975	0.161	0.977	0.546	0.978	0.483	0.978	0.492
Fe	0.0021	0.0193	0.0008	–	0.0021	0.025	0.0002	0.0002
Si	0.0009	0.0013	0.0003	0.0009	0.0011	0.0014	0.0012	0.0007
Cr	–	–	–	–	–	–	–	–
Ti	0.0001	–	0.0001	0.0001	–	–	–	–
Mn	0.0014	0.0013	0.0003	–	0.0001	0.0065	–	–
P	–	–	–	–	0.0003	–	–	–
Zn	–	–	–	–	0.0005	0.0003	0.0013	0.0002
O	1.000	1.000	1.000	1.000	1.000	1.000	1.000	1.000
Total	0.999	1.000	0.999	0.999	0.999	0.999	0.999	1.000

Table S2: Supplementary data. Chemical composition of marbles used for Sr-isotope analyses.

Sample	LLD	MR83	MR99	MR102	MR100	MR9	MR13	MR23b	MR26	MR27
SiO2	0.01 %	0.49	0.13	0.24	0.08	0.03	0.04	4.86	0.24	0.09
Al2O3	0.01 %	0.15	< 0.01	0.04	< 0.01	< 0.01	< 0.01	0.47	0.18	0.09
Fe2O3	0.01 %	0.08	0.03	0.06	0.02	< 0.01	< 0.01	0.29	0.01	< 0.01
MnO	0.01 %	0.01	0.01	0.02	0.01	0.01	0.01	0.09	0.01	0.01
MgO	0.01 %	0.34	0.40	0.37	15.85	0.46	0.51	16.88	0.92	0.61
CaO	0.01 %	53.59	53.79	53.39	31.00	54.69	54.66	28.77	53.59	53.88
Na2O	0.02 %	0.05	< 0.01	< 0.01	< 0.01	< 0.01	< 0.01	< 0.01	< 0.01	< 0.01
K2O	0.01 %	0.08	< 0.01	0.01	< 0.01	< 0.01	< 0.01	0.05	< 0.01	< 0.01
TiO2	0.01 %	0.02	< 0.01	< 0.01	< 0.01	< 0.01	< 0.01	0.01	< 0.01	< 0.01
P2O5	0.01 %	0.11	0.03	0.07	0.04	< 0.01	< 0.01	0.06	< 0.01	< 0.01
L.O.I.	0.01 %	n.d.	n.d.	n.d.	n.d.	n.d.	n.d.	n.d.	n.d.	n.d.
Total	- - - - -	54.92	54.39	54.20	47.00	55.19	55.22	51.48	54.95	54.68
As	1 ppm	< 1	< 1	< 1	< 1	< 1	< 1	< 1	< 1	< 1
Ba	10 ppm	< 10	< 10	< 10	< 10	< 10	< 10	< 10	< 10	< 10
Bi	1 ppm	< 1	< 1	< 1	< 1	< 1	< 1	< 1	< 1	< 1
Br	1 ppm	1	1	1	1	2	1	1	2	2
Cl	10 ppm	80	60	80	50	100	60	40	50	50
Co	1 ppm	< 2	< 2	< 2	< 2	< 2	< 2	< 2	< 2	< 2
Cr	1 ppm	6	6	5	5	< 2	2	4	3	< 1
Cu	1 ppm	4	< 1	< 1	3	< 1	< 1	2	2	2
Ga	1 ppm	< 1	< 1	< 1	< 1	< 1	< 1	< 1	< 1	< 1
Ge	1 ppm	< 1	< 1	< 1	< 1	< 1	< 1	< 1	< 1	< 1
Hf	1 ppm	< 1	< 1	< 1	< 1	< 1	< 1	< 1	< 1	< 1
Mo	1 ppm	< 1	< 1	< 1	< 1	< 1	< 1	< 1	< 1	< 1
Nb	1 ppm	< 1	< 1	< 1	< 1	< 1	< 1	< 1	< 1	< 1
Ni	1 ppm	< 1	< 1	< 1	< 1	< 2	< 2	4	< 1	< 1
Pb	1 ppm	4	3	3	2	5	5	3	2	3
Rb	1 ppm	4	1	1	< 1	1	1	2	1	1
S	10 ppm	50	60	60	140	70	40	20	40	50
Sb	3 ppm	< 3	< 3	< 3	< 3	< 3	< 3	< 3	< 3	< 3
Se	1 ppm	< 1	< 1	< 1	< 1	< 1	< 1	< 1	< 1	< 1
Sn	3 ppm	< 3	< 3	< 3	< 3	< 3	< 3	< 3	< 3	< 3
Sr	1 ppm	160	244	207	45	169	177	106	184	153
Ta	2 ppm	< 2	< 2	< 2	< 2	< 2	< 2	< 2	< 2	< 2
Th	1 ppm	4	4	2	1	< 1	2	1	3	3
Tl	1 ppm	< 1	< 1	< 1	< 1	< 1	< 1	< 1	< 1	< 1
U	1 ppm	< 1	< 1	< 1	< 1	< 1	< 1	< 1	< 1	< 1
V	2 ppm	6	< 2	6	< 2	< 2	< 2	8	< 2	< 2
W	2 ppm	< 1	< 1	< 1	< 1	< 1	< 1	< 1	< 1	< 1
Y	1 ppm	5	1	3	< 1	4	3	< 1	1	< 1
Zn	1 ppm	6	3	3	8	10	7	22	8	5
Zr	1 ppm	< 1	< 1	< 1	< 1	< 1	< 1	< 1	< 1	< 1

EDXRFA (Spectro-Xepos), calibration: SRMs – Lucas-Tooth-Modell, samples: glass discs and/or powder pellets

major elements as oxide wt. %, Fe as Fe_2O_3tot., trace elements in ppm, L.O.I. at 1000 °C/2h, analysis on dry basis (105 °C/24h)

L.O.I.=loss on ignition, LLD=Lower Limit of Detection, n.d.=not determined